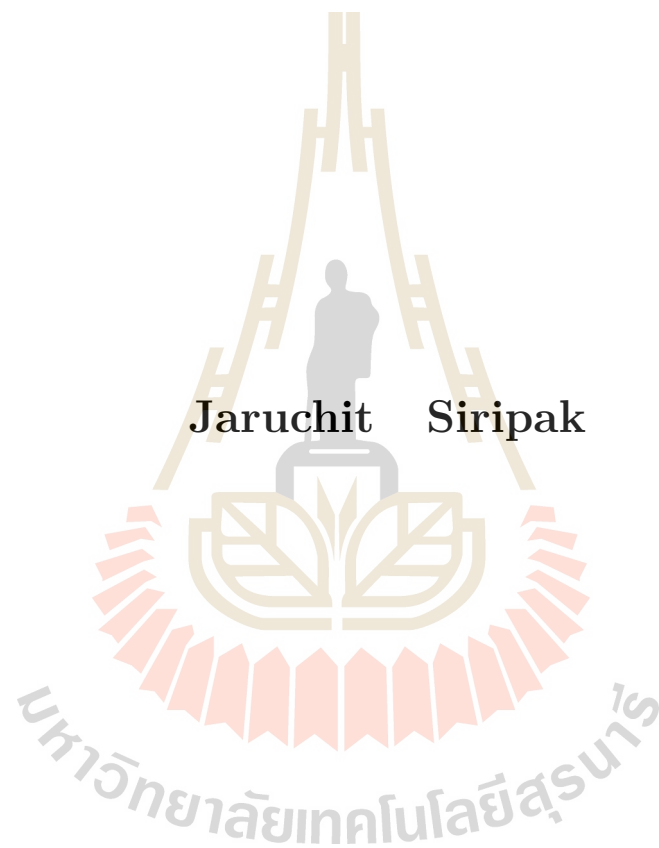


**A STUDY OF NEUTRINO SIGNAL FROM
DARK MATTER ANNIHILATION FOR
JUNO EXPERIMENT**



**A Thesis Submitted in Partial Fulfillment of the Requirements for the
Degree of Master of Science in Physics
Suranaree University of Technology
Academic Year 2018**

การศึกษาสัญญาณินวตริโนจากการประลัยของสสารมืดสำหรับการทดลอง

JUNO



นางสาวจารุจิตต์ ศิริภักดิ์

วิทยานิพนธ์นี้เป็นส่วนหนึ่งของการศึกษาตามหลักสูตรปริญญาวิทยาศาสตรมหาบัณฑิต

สาขาวิชาฟิสิกส์

มหาวิทยาลัยเทคโนโลยีสุรนารี

ปีการศึกษา 2561

**A STUDY OF NEUTRINO SIGNAL FROM DARK
MATTER ANNIHILATION FOR JUNO
EXPERIMENT**

Suranaree University of Technology has approved this thesis submitted in partial fulfillment of the requirements for a Master's Degree.

Thesis Examining Committee



(Assoc. Prof. Dr. Sirichok Jungthawan)

Chairperson



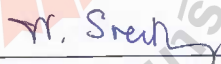
(Dr. Nuanwan Sanguansak)

Member (Thesis Advisor)



(Dr. Utane Sawangwit)

Member



(Dr. Warintorn Sreethawong)

Member



(Prof. Dr. Santi Maensiri)

Vice Rector for Academic Affairs
and Internationalization



(Assoc. Prof. Dr. Worawat Meevasana)

Dean of Institute of Science

จารุจิตต์ ศิริภักดิ์ : การศึกษาสัญญาณนิวตริโนจากการประลัยของสสารมืดสำหรับการทดลอง JUNO (A STUDY OF NEUTRINO SIGNAL FROM DARK MATTER ANNIHILATION FOR JUNO EXPERIMENT) อาจารย์ที่ปรึกษา : อาจารย์ ดร.นवलวรรณ สงวนศักดิ์, 61 หน้า.

สสารมืดมีบทบาทสำคัญในการก่อตัวของโครงสร้างขนาดใหญ่ในจักรวาลซึ่งอนุภาคสสารมืดที่ใช้ในการตรวจจับในปัจจุบันคือ Weakly Interacting Massive Particles (WIMPs) โดยคุณสมบัติของมันได้มาจากการสังเกตการณ์ทางดาราศาสตร์ อนุภาคชนิดนี้จะมีอันตรกิริยาอย่างอ่อนกับอนุภาคอื่นและสามารถสร้างอนุภาคในแบบจำลองมาตรฐาน เช่น $\tau^- \tau^+$, $u\bar{u}$, $e^- e^+$ เป็นต้น ผ่านการสลายตัวหรือการประลัยของตัวมันเอง ในการศึกษาครั้งนี้เราจะใช้ค่าภาคตัดขวางของการประลัยกันของ WIMPs $= 3 \times 10^{-26} \text{ cm}^2/\text{s}$ และกำหนดให้มวลของ WIMPs และความหนาแน่นของ WIMPs เป็นตัวแปรอิสระและยังสนใจแค่อนุภาคนิวตริโนในสถานะสุดท้ายที่ได้จากการประลัยกันของ WIMPs ที่ถูกจับไว้ในใจกลางของดวงอาทิตย์โดยใช้ซอฟต์แวร์ WimpSim ในการจำลองสเปกตรัมของนิวตริโน โดยคาดหวังว่า Jiangmen Underground Neutrino Observatory (JUNO) อาจจะตรวจจับมันได้ จำนวนของเหตุการณ์ของมันจะขึ้นอยู่กับมวลของ WIMPs และค่าภาคตัดขวางแบบพิจารณาสปินของสสารมืดและโปรตอน ($\sigma_{\chi p}^{SD}$) โดยกำหนดให้ความหนาแน่นของ WIMPs ในบริเวณระบบสุริยะเท่ากับ $0.3 \text{ GeV}/\text{cm}^3$ และความเร็วของ WIMPs $= 270 \text{ km/s}$ การทดลอง JUNO ที่ระดับ 2σ เมื่อทำการทดลองอย่างน้อย 5 ปี จะสามารถวัดค่า $\sigma_{\chi p}^{SD}$ อยู่ที่ประมาณ $7.8 \times 10^{-40} \text{ cm}^2$ สำหรับ WIMPs มวลระหว่าง $10 - 20 \text{ GeV}$ โดยพิจารณาผลของการประลัยกันของสสารมืดแล้วเกิด $\nu_e \bar{\nu}_e$ ทั้งนี้เราต้องการศึกษาผลของสัญญาณนิวตริโนพวกนี้รวมเข้ากับโครงร่างซอฟต์แวร์ของ JUNO เพื่อทำการเปรียบเทียบสัญญาณนี้ด้วยนิวตริโนที่มาจากปฏิกิริยาฟิวชันที่เกิดขึ้นในใจกลางดวงอาทิตย์และนิวตริโนจากชั้นบรรยากาศบนตัวตรวจจับ JUNO พบว่านิวตริโนที่มาจากปฏิกิริยาฟิวชันสามารถแยกออกจากสัญญาณของเราได้จากสเปกตรัมพลังงานและพลังงานที่เกิดขึ้นเมื่อนิวตริโนชนเข้ากับตัวตรวจจับ JUNO แต่เรายังไม่สามารถแยกนิวตริโนจากชั้นบรรยากาศได้ เนื่องจากมีการกระจายตัวของพลังงานและสัญญาณต่าง ๆ บน PMTs ที่คล้ายกัน แต่เราคาดหวังว่าการทำ vertex reconstruction อาจจะช่วยให้สามารถอธิบายได้

สาขาวิชาฟิสิกส์

ปีการศึกษา 2561

ลายมือชื่อนักศึกษา Jaruchit Siripak

ลายมือชื่ออาจารย์ที่ปรึกษา N. Sangwanrae

ลายมือชื่ออาจารย์ที่ปรึกษาร่วม Atta Saye

JARUCHIT SIRIPAK : A STUDY OF NEUTRINO SIGNAL FROM
DARK MATTER ANNIHILATION FOR JUNO EXPERIMENT.

THESIS ADVISOR : NUANWAN SANGUANSACK, Ph.D. 61 PP.

NEUTRINO/DARK MATTER/WIMPS/JUNO EXPERIMENT

Dark matter (DM) plays a major role in the large-scale structure formation of the universe. The leading candidate for DM particle is generally called Weakly Interacting Massive Particles (WIMPs) for its properties inferred from cosmological observations. Such DM particle would only interact via weak interaction and could decay or self-annihilate into other standard model particles such as $\tau\bar{\tau}, u\bar{u}, e^-e^+$, three flavor $\nu\bar{\nu}$. The thermal relic model predicts an upper limit of WIMPs annihilation cross section of $3 \times 10^{-26} \text{ cm}^3/\text{s}$ which is independent of the mass and such value has been ruled out for low mass DM particle $< \sim 10 \text{ GeV}$. We focus on the final-state neutrino particles from solar-captured WIMPs annihilation and expected signals at the Jiangmen Underground Neutrino Observatory (JUNO). The number of these events is related to the annihilation channel, mass of WIMPs, and spin-dependent WIMPs-proton interaction cross section (σ_{xp}^{SD}) by using local WIMPs density = $0.3 \text{ GeV}/\text{cm}^3$ and WIMPs dispersion velocity = 270 km/s . We found that the JUNO 5-years 2σ sensitivities is $\sigma_{xp}^{SD} = 7.8 \times 10^{-40} \text{ cm}^2$ for WIMPs in the mass range $10\text{--}20 \text{ GeV}$ from $\nu_\tau\bar{\nu}_\tau$ channel. Moreover, We integrate these neutrino signal resulting from captured WIMPs annihilation inside the solar core which is simulated by the WimpSim package to JUNO software framework for the detector simulation in order to compare these signal with the expected solar and atmospheric neutrino. Using the energy spectrum and deposited energy, the solar neutrino can be distinguished from the DM signal but the atmospheric

signal requires further investigations. For example, vertex reconstruction could be used to distinguish these different signal origins.



School of Physics

Academic Year 2018

Student's Signature Jasuchit Siripak

Advisor's Signature N. Sangsuan

Co-advisor's Signature [Signature]

ACKNOWLEDGEMENTS

First of all, I am totally grateful to my advisor, Dr. Nuanwan Sanguansak and my co-advisor, Dr. Utane Sawangwit for their suggestion and teaching physics in this work, helping me when I have problems and supporting me all the time.

Moreover, I would like to thank Assoc. Prof. Dr. Sirichok Jungthawan and Dr. Warintorn Sreethawong for sitting on the committee and giving advice to me.

I wish to thank Mr. Kittipong Wangnok, for always helping me everything when I ask him, and JUNO collaboration, for guiding and discussing the JUNO software framework. Furthermore, I appreciate every people who are not mentioned here that help me to finish this thesis.

I acknowledge the financial support from the Development and Promotion of Science and Technology talents project of Thailand (DPST) and partially supported from the Center of Excellence in high energy physics and astrophysics (CoE), Suranaree University of Technology.

Finally, I would especially like to thank my parents for their understanding and always supporting and encouraging all my life.

Jaruchit Siripak

CONTENTS

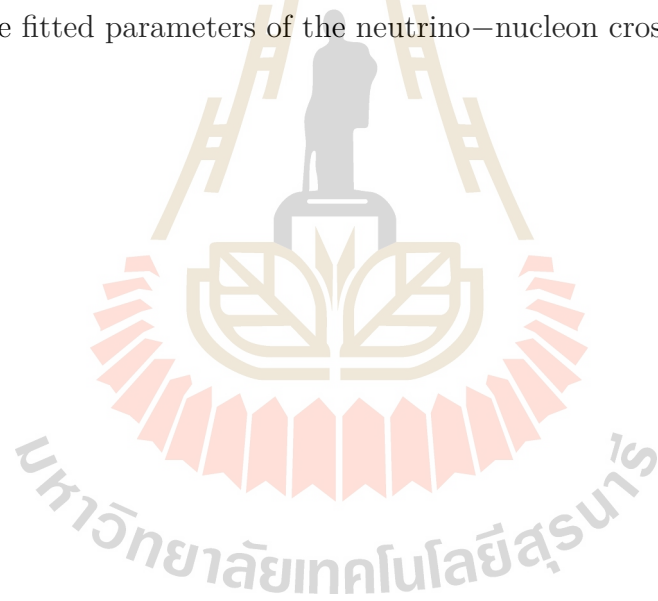
	Page
ABSTRACT IN THAI	I
ABSTRACT IN ENGLISH	II
ACKNOWLEDGEMENTS	IV
CONTENTS	V
LIST OF TABLES	VII
LIST OF FIGURES	VIII
LIST OF ABBREVIATIONS	XIV
CHAPTER	
I INTRODUCTION	1
II THEORY	5
2.1 Dark matter candidate	5
2.1.1 Axion	6
2.1.2 Sterile neutrino	7
2.1.3 Weakly interacting massive particles	7
2.2 The Potential DM source	9
2.3 Neutrino oscillation and neutrino interaction	13
2.3.1 Neutrino oscillation	13
2.3.2 Neutrino interaction	15
2.4 JUNO detector and JUNO software framework	17
2.4.1 JUNO detector	17
2.4.2 JUNO software framework	18

CONTENTS (Continued)

	Page
III METHODOLOGY	21
3.1 Calculation of neutrino event rate from WIMPs annihilation	21
3.1.1 WIMPs annihilation into neutrinos in the Milky Way galaxy	21
3.1.2 Solar captured WIMPs annihilation inside the Sun's core	23
3.2 Neutrino from solar captured WIMP annihilation on detector simulation	32
IV RESULT AND DISCUSSION	35
4.1 Result of neutrino event rate from WIMPs annihilation	35
4.1.1 The neutrino flux from WIMPs annihilation in the Milky Way galaxy	35
4.1.2 The neutrino flux from captured WIMPs annihilation inside the Sun's core	37
4.2 Result of neutrino from solar captured WIMPs annihilation on detector simulation	40
V CONCLUSION	54
REFERENCES	56
CURRICULUM VITAE	61

LIST OF TABLES

Table		Page
2.1	The fitted parameters for the DM density profile of the MW galaxy (Nesti and Salucci, 2013) (Wechakama and Ascasibar, 2014).	10
2.2	The best-fit neutrino oscillation parameters (An et al., 2016).	14
3.1	The local WIMPs density and velocity dispersion (Nesti and Salucci, 2013).	25
3.2	The fitted parameters of the neutrino-nucleon cross-sections.	30



LIST OF FIGURES

Figure		Page
1.1	The rotation curve of the MW galaxy plots between rotation speed and radius of MW. Each dotted is observation and the solid line is fitting data (Clemens, 1985).	2
1.2	The Bullet Cluster from X-ray observation show distribution of baryonic matter. The green contour plot is mass density. (Roszkowski et al., 2018).	3
2.1	Cross-section of DM interaction with ordinary matter as a function of DM particle's mass with different DM candidate. The red, pink and blue display HDM, WDM, and CDM, respectively (Roszkowski et al., 2018).	8
2.2	The DM density as a function of radius from GC, NFW (solid line), Burkert (dotted line) and Einasto (dotted-dashed line) profile. The dashed line represents the location of the Sun from GC at 8.5 kpc.	10
2.3	The WIMPs is captured by the gravitational force in the Sun's core. They can be annihilated with themselves into SM particles and eventually decay into neutrinos. These neutrinos propagate from the center of the Sun to neutrino telescopes on the Earth.	11
2.4	The layout of the WimpSim program with the two main parts WimpAnn and WimpEvent (Edsjo and Niblaeu, 2017).	12

LIST OF FIGURES (Continued)

Figure		Page
2.5	The total neutrino–electron scattering cross section as a function of neutrino energy.	16
2.6	Schematic view of JUNO detector (Wurm, 2017).	18
2.7	Offline Processing Full Chain (Lin, 2016).	19
2.8	Offline Processing inside tut_detsim.py.	20
3.1	The annihilation rate with different MW DM halo profile which gives the different value of local density and dispersed velocity and using the $\sigma_{\chi\bar{\chi}}^{SD} = 10^{-39} \text{cm}^2$. The dashed line uses NFW profile. The dotted line uses Einasto profile. The solid line uses Burkert profile. The dotted–dashed line is the fiducial model with $\rho_0 = 0.3 \text{ GeV}/\text{cm}^3$ and $\bar{v} = 270 \text{ km/s}$	26
3.2	The electron neutrino spectrum with the ratio of neutrino energy (E_ν) and mass of WIMPs (m_χ) by using 10 GeV in the Sun’s core for an upper figure and 1 AU for a lower figure. Each of the color lines is different particle channels from DM annihilation.	27
3.3	The electron neutrino spectrum with the ratio of neutrino energy (E_ν) and mass of WIMPs (m_χ) by using 1 TeV in the Sun’s core for an upper figure and 1 AU for a lower figure. Each of the color lines is different particle channels from DM annihilation.	28
3.4	The error of the parameterizations (in %) of the total cross–sections with different interaction as a function of neutrino energies in GeV (Edsjo, 2007).	31

LIST OF FIGURES (Continued)

Figure		Page
3.5	The total cross-section as a function neutrino energy in GeV. The dotted-dashed line is a total neutrino-proton cross-section via CC. The dotted line is a total neutrino-proton cross-section via NC. The dashed line is a total neutrino-neutron cross-section via CC. The solid line is a total neutrino-neutron cross-section via NC.	32
3.6	The scheme of solar neutrino generator. The val = Uniform-Rand() and $\sigma(E_\nu, E_e)$ is a normalized cross-section.	33
4.1	The differential neutrino flux from GC with Burkert profile and each color lines presents WIMPs mass between 20 MeV to 60 MeV.	36
4.2	The number of neutrino per neutrino energy (dN/dE) using Burkert profile, WIMPs mass in a range 20 MeV-60 MeV, IBD cross-section and time exposure 10 years	37
4.3	The number of electron neutrinos per its energy (dN/dE) with WIMPs mass 10 GeV, consider neutrino-nucleon scattering cross-section and integration time 1 year. The blue line is from $\tau^- \tau^+$ channel and the orange line is from $\nu_\tau \bar{\nu}_\tau$ channel.	38
4.4	The number of electron neutrinos per its energy (dN/dE) with WIMPs mass 100 GeV, consider neutrino-nucleon scattering cross-section and integration time 1 year. The blue line is from $\tau^- \tau^+$ channel and the orange line is from $\nu_\tau \bar{\nu}_\tau$ channel.	39

LIST OF FIGURES (Continued)

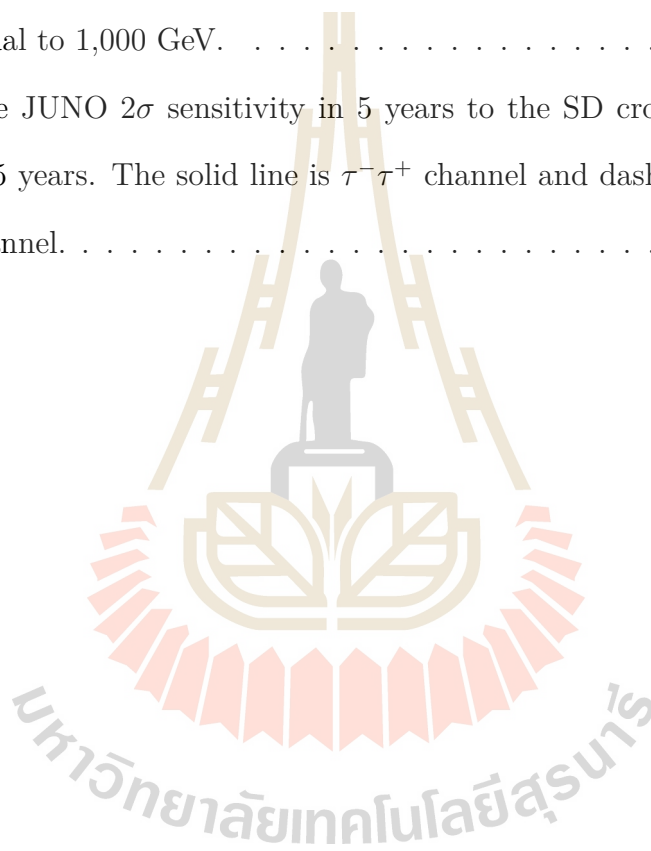
Figure		Page
4.5	The number of electron neutrinos per its energy (dN/dE) with WIMPs mass 1,000 GeV, consider neutrino–nucleon scattering cross–section and integration time 1 year. The blue line is from $\tau^-\tau^+$ channel and the orange line is from $\nu_\tau\bar{\nu}_\tau$ channel.	39
4.6	The histogram of the total number of PE from capture WIMPs mass equal to 10 GeV and $\tau^-\tau^+$ annihilated channels with blue histogram is ν_x and orange histogram is ν_e	41
4.7	The histogram of the total number of PE from captured WIMPs mass equal to 10 GeV. The mean of PE numbers is 6.61×10^6 and the standard deviation of this plot is 4.43×10^6	42
4.8	The histogram of the total number of PE from atmospheric neutrino. The mean of PE numbers is 1.47×10^6 and the standard deviation of this plot is 2.13×10^6	42
4.9	The histogram of the total number of PE from solar neutrino channel Be8. The mean of PE numbers is 5.62×10^3 and the standard deviation of this plot is 4.09×10^3	43
4.10	The histogram of the total number of PE in each event and from different sources, blue: atmospheric neutrino, orange: WIMPs mass equal to 10 GeV, and green: solar neutrino (channel Be8) .	43

LIST OF FIGURES (Continued)

Figure		Page
4.11	The histogram of deposited energy in MeV from captured WIMPs mass equal to 10 GeV. The mean energy of deposition is 4.35×10^3 MeV and the standard deviation of this plot is 2.88×10^3 MeV.	45
4.12	The histogram of deposited energy in MeV from atmospheric neutrino. The mean energy of deposition is 1.04×10^3 MeV and the standard deviation of this plot is 1.48×10^3 MeV.	45
4.13	The histogram of deposited energy from solar neutrino channel Be8. The mean energy of deposition is 4.71 MeV and the standard deviation of this plot is 2.66 MeV.	46
4.14	The histogram of deposited energy in MeV from different sources, blue: atmospheric neutrino, orange: WIMPs mass equal to 10 GeV, and green: solar neutrino (channel Be8)	46
4.15	The histogram of hit time of PE hitting PMT in nanosecond from captured WIMPs mass equal to 10 GeV. The mean of hit time is 1.5×10^8 nanoseconds and the standard deviation is 5.91×10^{10} nanoseconds.	48
4.16	The histogram of hit Time of PE hitting PMT in nanosecond from an atmospheric neutrino. The mean of hit time is 1.75×10^{17} nanoseconds and the standard deviation is 1.17×10^{20} nanoseconds.	48
4.17	The histogram of hit Time of PE hitting PMT in nanosecond from solar neutrino channel Be8. The mean of hit time is 1.06×10^2 nanoseconds and the standard deviation is 81.9 nanoseconds.	49

LIST OF FIGURES (Continued)

Figure		Page
4.18	The histogram of deposited energy from captured WIMPs mass equal to 100 GeV.	50
4.19	The histogram of deposited energy from captured WIMPs mass equal to 1,000 GeV.	51
4.20	The JUNO 2σ sensitivity in 5 years to the SD cross section $\sigma_{\chi P}^{SD}$ in 5 years. The solid line is $\tau^-\tau^+$ channel and dashed line is $\nu_\tau\bar{\nu}_\tau$ channel.	52



LIST OF ABBREVIATIONS

CC	Charge Current
CD	Central Detector
CDM	Cold Dark Matter
CDMS	Cryogenic Dark Matter Search
CMB	Cosmic Microwave Background
CP	Charge Parity
DM	Dark Matter
edep	Deposited Energy
Fermi–LAT	Fermi–Large Area Telescope
HDM	Hot Dark Matter
H.E.S.S.	High Energy Stereoscopic System
hitTime	Hit Time
IAU	International Astronomical Union
IH	Inverse Hierarchy
GC	Galactic Center
JUNO	Jiangmen Underground Neutrino Observatory
KK	Kaluza–Klein
LHC	Large Hadron Collider
LS	Liquid Scintillator
LSP	Lightest Supersymmetry Particle
LSS	Large Scale Structure
MC	Monte–Carlo

LIST OF ABBREVIATIONS (Continued)

MW	Milky Way
NC	Neutral Current
NFW	Navarro–Frenk–White
NH	Normal Hierarchy
NPP	Nuclear Power Plant
PE	PhotoElectron
PAMELA	Payload for Antimatter Matter Exploration and Light–nuclei Astrophysics
QCD	Quantum ChromoDynamics
SD	Spin–Dependent
SI	Spin–Independent
SM	Standard Mode
SN	SuperNova
SNiPER	Software for Non–collider Physics Experiment
PMTs	PhotoMultiplier Tubes
WDM	Warm Dark Matter
WIMPs	Weakly Interacting Massive Particles
ZEPLIN	ZonEd Proportional scintillation in LIquid Noble gases

CHAPTER I

INTRODUCTION

The universe is gargantuan and consists of numerous stars, galaxies, clusters and many mysterious things whose phenomena cannot be explained; thus there are various interesting topics to study. The advanced technology and new knowledge occur during a study of the universe such as new telescopes and sensitive system to detect light from distant objects and separate the signal from the background (BG) and the foreground signal. From N-body simulation and PLANCK, Cosmic Microwave Background (CMB) data, it has been shown that the abundance of the universe's matter-energy components are 69% dark energy, 27% dark matter, and remaining 4% ordinary matter. Dark energy is an unknown energy which causes accelerated universe's expansion. Dark matter (DM) is the invisible matter or non-baryonic matter which has very little or no interaction with other components except through gravity. The ordinary matter is a normal matter or baryonic matter such as dust, elementary atom, the Sun and the Earth (Majumdar, 2015).

Up to now, there have not been any report of detecting the DM particle and their properties are unclear. They are a significant part of Large Scale Structure (LSS) of the universe. The stars, galaxies, and cluster are made up by them. Their clumping can create the gravitational force and pull the gas, dust, and atoms to form bigger objects (Majumdar, 2015). In 1933, Fritz Zwicky proposed the term of non-luminous matter "Dark Matter" from his measurement of the velocity dispersion of galaxies in the Coma cluster (Goodstein, 2012). He found that the total luminous object is not enough to elucidate his observation. Later, Vera Rubin

et al. studied the rotation curve of galaxies and found that observed velocity of an object at large radii is much higher than the one that predicted by Newtonian Mechanics. The example of Milky Way (MW) rotation curve is shown in Figure 1.1. From 2nd Newtonian law and gravitational force, the object velocity should be decreased with distance from the Galactic Center (GC), but the observation shows that the rotation curve is approximately flat at large distance. That means, there should be some invisible mass which can be interpreted as existence of DM.

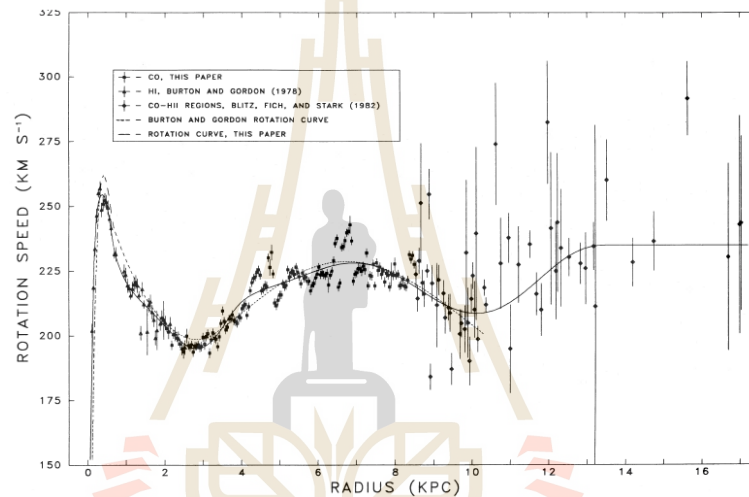


Figure 1.1 The rotation curve of the MW galaxy plots between rotation speed and radius of MW. Each dotted is observation and the solid line is fitting data (Clemens, 1985).

Another DM evidence is by the observation of galaxy cluster collision with X-ray and gravitational lensing in Figure 1.2. The X-ray observation traces hot plasma gas and dust interaction and the gravitational lensing traces the DM distribution which moves pass each other and is less interaction with dust or gas. The gravitational lensing can detect DM by light rays from far galaxies which can be distorted when passing through massive bodies due to curvature of space-time (Roszkowski et al., 2018).

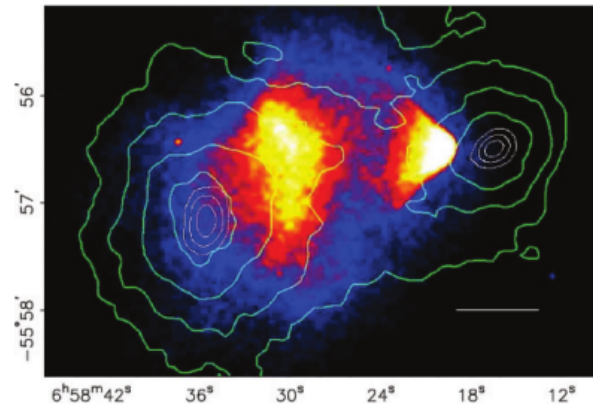
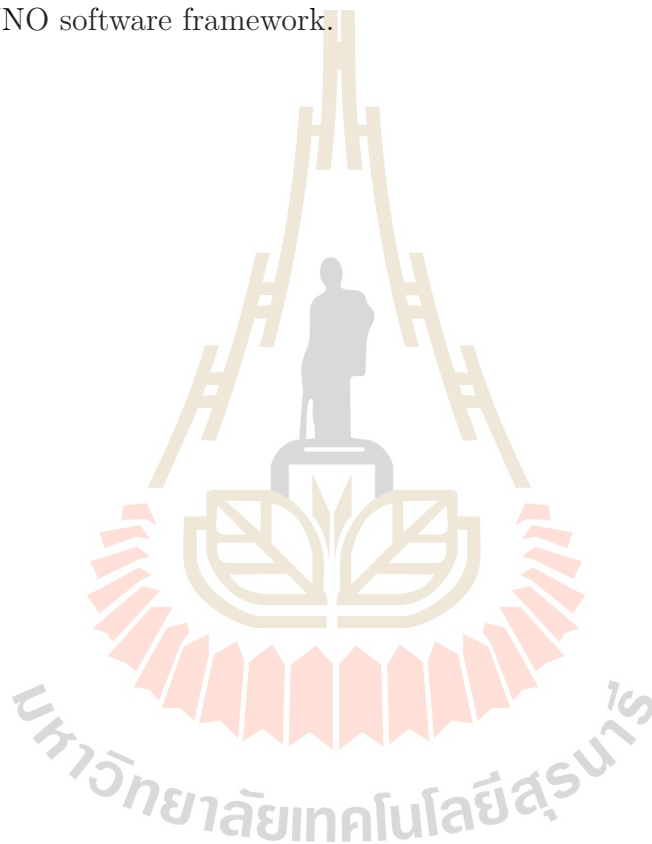


Figure 1.2 The Bullet Cluster from X-ray observation show distribution of baryonic matter. The green contour plot is mass density. (Roszkowski et al., 2018).

The DM does not interact or weakly interact with other matter. This is the reason why they still are not detected. The strategies to study DM are divided into 3 ways. Firstly, direct detections are expected to detect the DM particles that collide with nuclei of noble gas in the detector and produce the photon to hit PhotoMultiplier Tubes (PMTs) such as XENON dark matter research project, ZonEd Proportional scintillation in LIquid Noble gases (ZEPLIN), and Cryogenic Dark Matter Search (CDMS) (Goodstein, 2012). Secondly, indirect detections search the production from DM annihilation or decay from the whole sky e.g. gamma-ray, neutrino, and electron-positron. The examples of a telescope are Fermi-Large Area Telescope (Fermi-LAT) to collect gamma-ray, Jiangmen Underground Neutrino Observatory (JUNO) to detect neutrinos, Payload for Antimatter Matter Exploration and Light-nuclei Astrophysics (PAMELA) to seek cosmic ray particularly antimatter: positron and antiproton, and High Energy Stereoscopic System (H.E.S.S) which is ground-based telescope to obtain high energetic photon in gamma-ray wavelength. Finally, search for DM in Large Hadron Collider (LHC) that allow two protons to collide each other and find missing momentum and energy which has also detect nothing.

In this work, we are interested in indirect detection and we would like to study neutrinos as the final state particle from the DM annihilation for JUNO. In the JUNO Yellowbook (An et al., 2016), they proposed to simulate the neutrino from captured DM inside the Sun's core but their results do not include a JUNO detector simulation which takes the experiment sensitivity and other BG events into account. Therefore, in this work, we would like to investigate the results by including JUNO software framework.



CHAPTER II

THEORY

This chapter is devoted to review DM candidates, DM sources, JUNO detector and its software framework, and neutrino oscillation and interaction with Liquid Scintillator (LS). The promising of DM candidate is presented in section 2.1. The DM signal mostly comes from the Galactic Center (GC) due to the dense of DM density. Nevertheless, the Sun can capture DM particles and their self-annihilation in the Sun's core will be explained in section 2.2. The DM annihilation can produce neutrino particles that are detectable at the JUNO experiment. Section 2.3 describes the neutrino propagation and neutrino oscillation to the Earth and JUNO detector where the neutrino will interact with LS. Section 2.4 shows the detail about JUNO detector and JUNO software framework used to simulate the neutrino signal.

2.1 Dark matter candidate

Many cosmological observations and simulations support and require the DM existence. However, none of experiments have discovered the DM particle. There are many theoretical models of DM particle to predict exact properties and its interaction corresponding to observations. PLANCK and power spectrum express roughly of DM properties. Firstly, it is cold or non-relativistic and massive which can form LSS. The second property, it is stable and neutral which they can exist from an early universe to present and their lifetime is $10^{25} - 10^{26}$ second ($\sim 10^{19}$ year) for WIMPs mass equal to 100 GeV that is more than the age of the

universe (10^{10} year). The DM is a non-baryonic matter according to PLANCK data. The fourth property is the weak interaction with other matter (Drees and Gerbier, 2015). The DM density is obtained by measurement of the anisotropy of CMB and spatial distribution of galaxies (An et al., 2016). The fraction of DM density to the critical density is

$$\Omega_{DM}h^2 = 0.1198 \pm 0.0026 \quad (2.1)$$

where $h = 0.673 \pm 0.012$ is the Hubble constant. After freeze-out, the upper limit of average DM annihilation cross-section with a relative velocity of two DM particles in the center-of-mass frame (v) is expected from thermal relic model which satisfies in equation (2.2) (Roszkowski et al., 2018)

$$\langle\sigma v\rangle_{\chi\chi} = 3 \times 10^{-26} \text{ cm}^3/s \quad (2.2)$$

where χ means DM particle.

The DM candidates are separated into 3 main groups using their velocity: Hot Dark Matter (HDM) which is relativistic and is ruled out by LSS and CMB experiments, Warm Dark Matter (WDM), and Cold Dark Matter (CDM) which is non-relativistic. The currently leading DM candidates, namely, Axion, Sterile Neutrino, and Weakly Interacting Massive Particles (WIMPs) are presented as following.

2.1.1 Axion

It is raised to solve a strong Charge Parity (CP) problem in Quantum Chromodynamics (QCD) which can explain the QCD uphold CP-symmetry (Overduin and Wesson, 2008). The strong CP problem is why a value of Θ is very small and does not violate charge conservation and mirror symmetry. The Θ is

a free parameter and dimensionless in QCD. The answer of this “fine-tuning” problem is similar to the cosmological constant (Λ). Axion’s properties are cold, have consistent density with relic DM density and decay into photon pair (Drees and Gerbier, 2015). The Axion mass is very tiny around $0.01 \text{ eV}/c^2$ but it also can be a CDM because it is produced in non-thermal process (Drees and Gerbier, 2015).

2.1.2 Sterile neutrino

A hypothetical particle proposed as a right-handed neutrino candidate which has mass in the range between around 1 keV to 10^{15} GeV and only interact via gravity. If they are generated in the non-thermal process, they will decay into a photon and three flavor of neutrino (Drees and Gerbier, 2015). However, its relic density is not enough and cannot be formed the number of stars and galaxies at the present.

2.1.3 Weakly interacting massive particles

The properties of Weakly Interaction Massive Particle (WIMPs) represent in its name, weak interacting and massive in GeV-TeV range (Drees and Gerbier, 2015). It is predicted by conservation of R-parity in SuperSYmmetry (SUSY) model beyond Standard Model (SM), R-parity for SM particle = 1 and SUSY particle = - 1. The leading WIMPs in SUSY model is the Lightest Supersymmetric particle (LSP) that is massive, stable and neutral such as sneutrino and neutralino (An et al., 2016) but sneutrino is eliminated by a component of DM halo (Drees and Gerbier, 2015). Furthermore, WIMP can be gravitino (superpartner of graviton), bino (superpartner of gauge boson), higgsino (superpartner of higgs bosons) and axino (superpartner of axion) (Widmark, 2016). In a uni-

versal extra dimension (5th dimension) model presents the DM candidate in the excited Kaluza–Klein (KK) state (Overduin and Wesson, 2008). The SM particle is provided in the lowest state. The only KK state of DM candidate annihilate into directly three–flavor of neutrinos (An et al., 2016).

The best motivated DM candidate is CDM as their properties but a simulation shows that the structure in the universe should have more halo mass than at the present which causes a missing satellites problem. The WDM is suggested to solve this problem by reducing the power spectrum of CMB. In this thesis, we use WIMPs generally for DM particle candidate. Figure 2.1 presents various DM candidates with their range of masses and interacted cross sections.

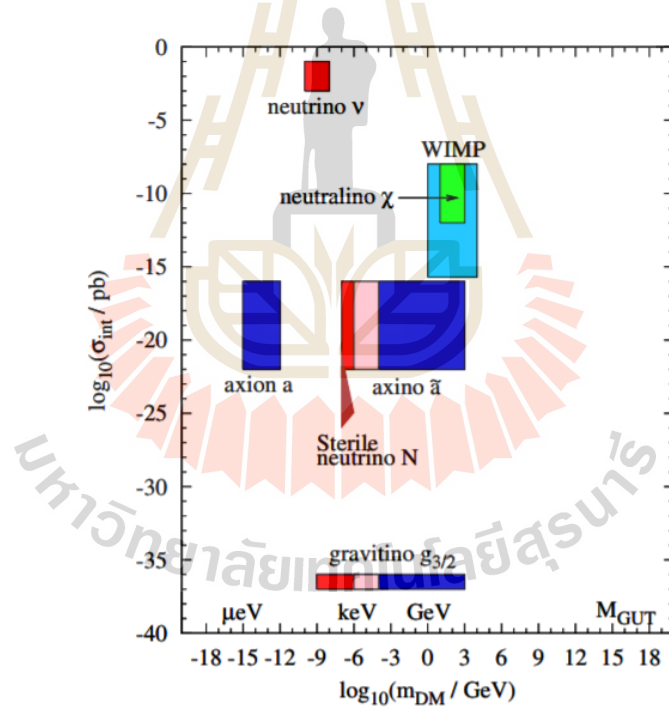


Figure 2.1 Cross–section of DM interaction with ordinary matter as a function of DM particle’s mass with different DM candidate. The red, pink and blue display HDM, WDM, and CDM, respectively (Roszkowski et al., 2018).

2.2 The Potential DM source

The WIMPs are distributed in all direction in the DM halo which is embedded in the MW galaxy. The highest DM density is located at the GC thus it is higher probability of self–annihilation than every area. Although the signal is very difficult to distinguish between the WIMPs signal and the other sources near GC such as the pulsars, the supernova remnant, and the interstellar medium. Bartels et al. (2017) presented the fitting of the excess gamma–ray from GC with a stellar mass profile and found that this emission results from stellar source population in GC. Nevertheless, there remains an unsolved diffuse signal that is interpreted as the WIMPs annihilation signal. The strength of the DM signal refer to DM number density or DM density profile and annihilation cross–section. Examples of DM density profiles are Navarro–Frenk–White (NFW) profile which is predicted from N–body simulation, and Einasto (1995) and Burkert profiles which are coming from fitting with astrophysical observation. Three DM density profiles are described using the following equations: NFW profile in equation 2.3 (Nesti and Salucci, 2013), Einasto profile in equation 2.4 from Einasto(1965), and Burkert profile in equation 2.5 (Nesti and Salucci, 2013).

$$\rho_{NFW} = \frac{\rho_H}{x(1+x)^2} \quad (2.3)$$

$$\rho_{Einasto} = \rho_H \exp\left[\frac{-2}{\alpha}(x^\alpha - 1)\right] \quad (2.4)$$

$$\rho_{Burkert} = \frac{\rho_H}{(1+x)(1+x^2)} \quad (2.5)$$

where $x = \frac{r}{R_H}$, r is radius from GC, ρ_H and R_H are fitted parameters of each model is shown in Table 2.1.

Table 2.1 The fitted parameters for the DM density profile of the MW galaxy (Nesti and Salucci, 2013) (Wechakama and Ascasibar, 2014).

Parameters	NFW	Einasto	Burkert
$\rho_H [10^7 \frac{M_\odot}{kpc^3}]$	1.40	0.16	4.13
$R_H [kpc]$	16.10	20.00	9.26
α	-	0.17	-

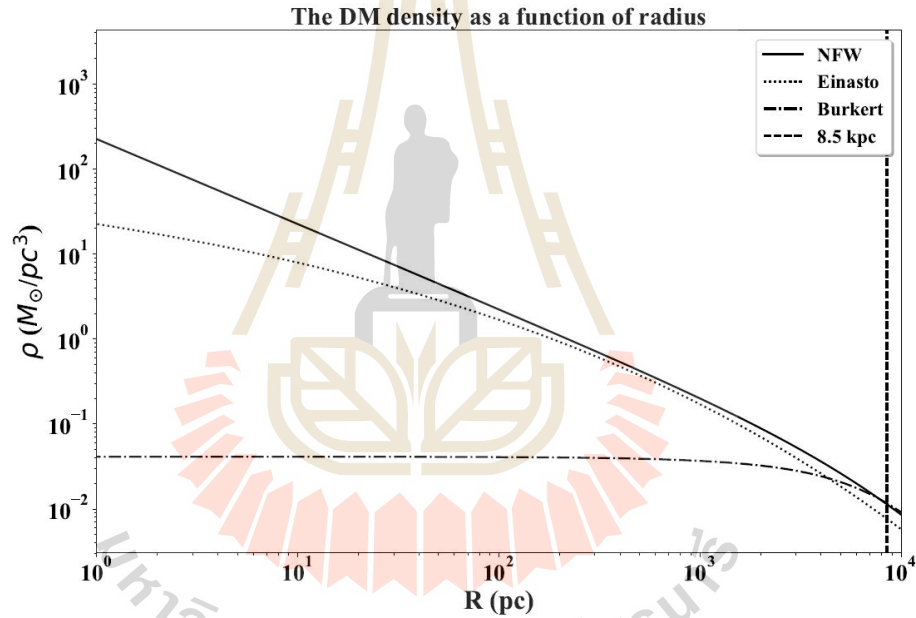


Figure 2.2 The DM density as a function of radius from GC, NFW (solid line), Burkert (dotted line) and Einasto (dotted–dashed line) profile. The dashed line represents the location of the Sun from GC at 8.5 kpc.

Figure 2.2 shows that the NFW profile provides a high density at close GC, while Einasto and Burkert profiles give finite density at GC. This disagreement is called the “core–cusp problem”. The cored profile has a flat density at small radii near GC and the cusped profile is diverge at small Galactic radii. In the

observation near GC has a lot of emissions that we can not fit the DM density profile in this area (Wechakama, 2013). However, the recently observational data constrained at a radius more than 2 kpc are consistent with the cored profile (Nesti and Salucci, 2013).

In addition, another potential area to study WIMPs is the Sun. The WIMPs can be captured by the gravity of the Sun. The captured WIMPs sink, accumulate in the Sun's core and annihilate into SM particles and photons shown in Figure 2.3. The Sun is closed to the Earth and this WIMPs annihilation signal can reduce the foreground signal as an effect from the interstellar medium. Therefore, the Sun is one of the interesting regions to investigate the DM.

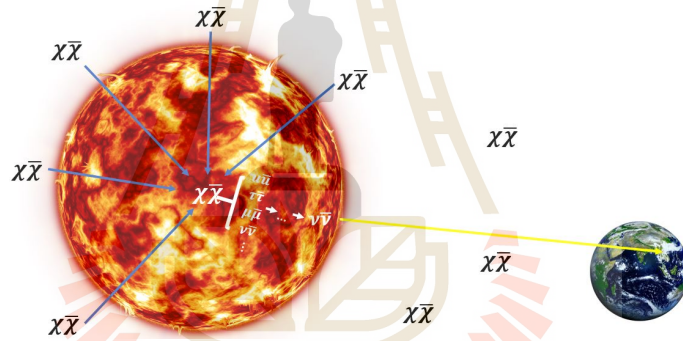


Figure 2.3 The WIMPs is captured by the gravitational force in the Sun's core. They can be annihilated with themselves into SM particles and eventually decay into neutrinos. These neutrinos propagate from the center of the Sun to neutrino telescopes on the Earth.

In this work, we focus on the captured of WIMPs in the solar core, three flavor of neutrino and antineutrino (ν_{e^-} , ν_{μ} , ν_{τ} , $\bar{\nu}_{e^-}$, $\bar{\nu}_{\mu}$, $\bar{\nu}_{\tau}$) from WIMPs annihilation. We use the WimpSim package (Edsjo and Niblaeu, 2017) to generate these neutrino spectra and the package includes an effect from the neutrino oscillation and interaction when neutrinos propagate from the center of the Sun to the Earth which will be discussed in the next section. This package considers DM's mass in

the range of GeV–TeV corresponding with the WIMPs DM candidate. In Figure 2.4 illustrate the layout of WimpSim package which consists of the WimpAnn and WimpEvent.

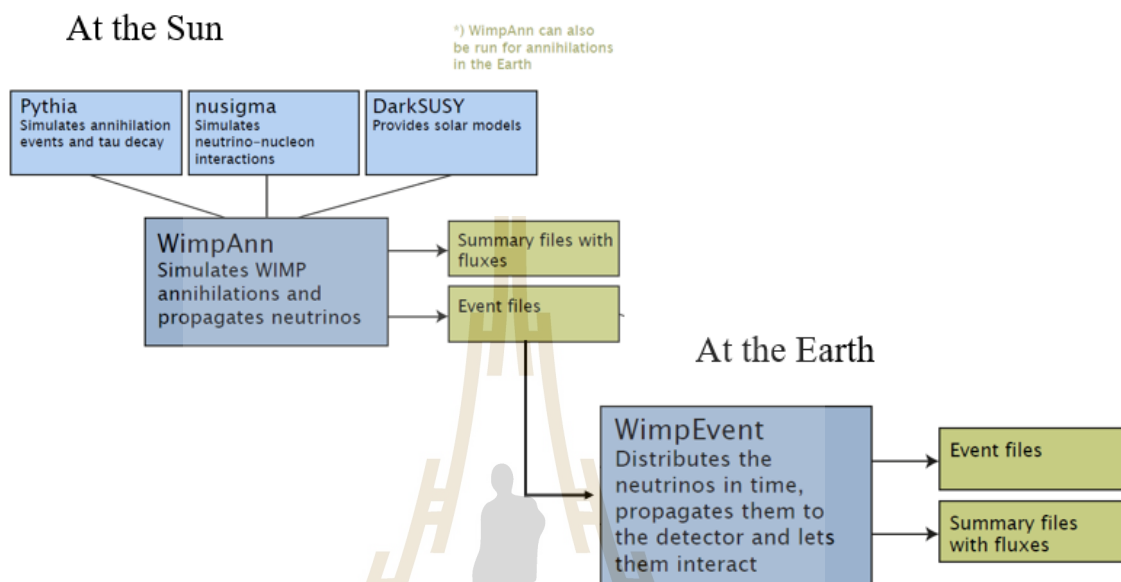


Figure 2.4 The layout of the WimpSim program with the two main parts WimpAnn and WimpEvent (Edsjo and Niblaeu, 2017).

The WimpAnn is one of the main program in WimpSim uses for generating WIMPs spectrum from the Sun's core and gather multiple external programs. The external programs are Pythia, generating an annihilation event, nusigma, calculating neutrino–nucleon interaction inside the Sun, and DarkSUSY, considering solar model for time evolution in neutrino oscillation. The WimpEvent is another program for simulating neutrino propagate at 1 AU to a specific detector by latitude and longitude, random time stamp and selected interaction and target (water or rock). The WimpEvent needs an inputted event file from WimpAnn, thus we have to run the WimpAnn first. Besides the WimpSim can simulate the captured WIMPs by the gravity of Earth but the events are so small.

2.3 Neutrino oscillation and neutrino interaction

The universe composes of a lot of celestial objects and radiation that can produce the neutrinos. The notable properties of neutrino are relativistic and weakly interacting which it can be traced back to the source similar to the gamma-ray and the source may be identified. This section is dedicated to only neutrino theory for this thesis. The neutrino oscillation is described in section 2.3.1. They can change their type to another type when they arrive at the Earth and hit LS in a detector, they can produce charged particles and release energy. The neutrino telescope can detect neutrino consequently by these particles and energy. The different neutrino interaction allows different charged particles and energy range which will be discussed in section 2.3.2.

2.3.1 Neutrino oscillation

The neutrino oscillation discovery obtained Nobel prize in 2015. This phenomenon notifies that neutrino can change lepton flavor and refers that the neutrino is not massless. The neutrino oscillation depends on the neutrino flavor eigenstate and it is a linear combination of mass eigenstate which can be written as (Blennow et al., 2008)

$$|\nu_\alpha\rangle = \sum_a U_{\alpha a}^* |\nu_a\rangle \quad (2.6)$$

where $|\nu_\alpha\rangle$ ($\alpha = e, \mu, \tau$) is a neutrino flavor eigenstate, $|\nu_a\rangle$ ($a = 1, 2, 3$) is the neutrino mass eigenstates with definite masses m_a , and U is the leptonic mixing matrix which is unitary matrix and expressed in standard parameters by equation

(2.7).

$$U = \begin{bmatrix} c_{12}c_{13} & s_{12}c_{13} & s_{13}e^{-i\delta} \\ -s_{12}c_{23} - c_{12}s_{13}s_{23}e^{i\delta} & c_{12}c_{23} - s_{12}s_{13}s_{23}e^{i\delta} & c_{13}s_{23} \\ s_{12}s_{23} - c_{12}s_{13}c_{23}e^{i\delta} & -c_{12}s_{23} - s_{12}s_{13}c_{23}e^{i\delta} & c_{13}c_{23} \end{bmatrix} \quad (2.7)$$

where $c_{ij} \equiv \cos\theta_{ij}$ and $s_{ij} \equiv \sin\theta_{ij}$ (for $ij = 12, 13, 23$). The neutrino oscillation parameters are given in Table 2.2.

Table 2.2 The best-fit neutrino oscillation parameters (An et al., 2016).

Parameters	Normal Hierarchy (NH)	Inverse Hierarchy (IH)
$\Delta m_{21}^2/10^{-5}eV^2$	7.54	7.54
$\Delta m_{31}^2/10^{-3}eV^2$	2.47	2.42
$\sin^2\theta_{12}/10^{-1}$	3.08	3.08
$\sin^2\theta_{13}/10^{-2}$	2.34	2.40
$\sin^2\theta_{23}/10^{-1}$	4.37	4.55
$\delta/180^\circ$	1.39	1.31

The probability of neutrino oscillation from $\nu_\alpha \rightarrow \nu_\beta$ ($P_{\nu_\alpha \rightarrow \nu_\beta}$) for $\alpha, \beta = e, \mu, \tau$ and $i, j = 1, 2, 3$ with distance (L) is calculated by (An et al., 2016)

$$P_{\nu_\alpha \rightarrow \nu_\beta} = \frac{\sum_i |U_{\alpha i}|^2 |U_{\beta i}|^2 + 2\sum_{i < j} [\text{Re}(U_{\alpha i}U_{\beta i}U_{\alpha i}^*U_{\beta i}^*)\cos\Delta_{ij} - \frac{(UU^\dagger)_{\alpha\alpha}(UU^\dagger)_{\beta\beta}}{\text{Im}(U_{\alpha i}U_{\beta i}U_{\alpha i}^*U_{\beta i}^*)\sin\Delta_{ij}}]}{(UU^\dagger)_{\alpha\alpha}(UU^\dagger)_{\beta\beta}} \quad (2.8)$$

where $\Delta_{ij} \equiv \Delta m_{ij}^2 L/(2E_\nu)$ and E_ν is neutrino energy. When the neutrino propagate from the solar core to the Earth, the evolution of the neutrino state is calculated by

$$|\nu(t)\rangle = S(t)|\nu(0)\rangle \quad (2.9)$$

where the evolution operator $S(t)$ depends on the distance and medium traversed

which refer to the number of the electron in the matter. The neutrino propagation from the solar core to the solar surface is obtained by using the solar model (Bahcall et al., 2005) to give approximate electron number density profile in each constant electron number density layer. In the vacuum, the electron number density is zero.

2.3.2 Neutrino interaction

When the neutrinos pass through the detector, they might interact with atoms in LS. The neutrino interaction has two types that are Charge Current (CC) and Neutral Current (NC). These transfer momentum and energy to the particle in LS. Moreover, the CC interaction will produce charge particles after colliding. The mediator exchange of CC and NC are W^+W^- and Z^0Z^0 , respectively. The number of neutrino events on the detector is related to the total neutrino interaction cross-section. The LS consists of many protons and neutrons. Therefore we will consider neutrino-proton and neutrino-neutron scattering cross section via CC and NC interactions. The differential cross section is set by a fraction of the nucleon's momentum and energy and spin symmetry of down and up quark (Edsjo, 2007). Furthermore the neutrinos occasionally elastic scatter off the electrons, the differential cross-section is given by (Bahcall et al., 1995)

$$\begin{aligned} \frac{d\sigma}{dT} = \frac{2G_F^2 m_e}{\pi} \{ & g_L^2(T) [1 + \frac{\alpha}{\pi} f_-(z)] + g_R^2(T) (1-z)^2 [1 + \frac{\alpha}{\pi} f_+(z)] \\ & - g_R(T) g_L(T) \frac{m_e}{z} [1 + \frac{\alpha}{\pi} f_{-+}(z)] \} \end{aligned} \quad (2.10)$$

where m_e is electron mass, $T = E - m_e$ is kinetic recoil electron energy, q is the neutrino energy and $z = T/q$. For obtaining other parameters, we can see more in Bahcall et al. (1995). The neutrino-electron scattering cross section depends on neutrino energy and kinetic recoil electron energy. The higher neutrino energy

provide the high total cross-section as shown in Figure 2.5.

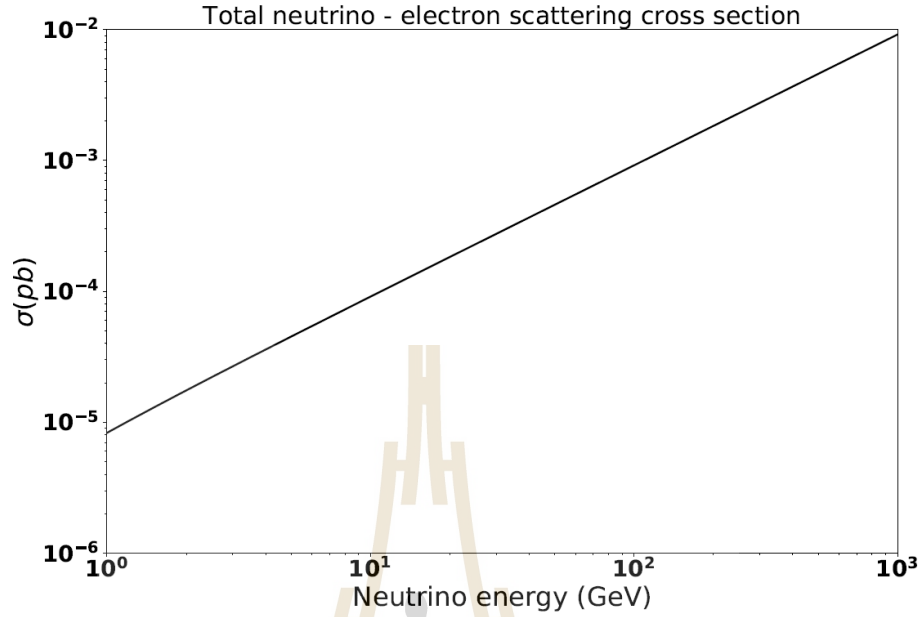


Figure 2.5 The total neutrino–electron scattering cross section as a function of neutrino energy.

The main neutrino interaction with the LS for low-energy neutrino ($E_\nu \lesssim 60$ MeV) is Inverse Beta Decay (IBD). The lower neutrino energy for IBD is 1.8 MeV. When the electron antineutrino hit proton and then produce the positron and the neutron, the positron can be annihilated with the electron in LS and generate gamma-ray, 511 keV, which is called “prompt signal”. The neutron can be captured by nuclei after prompt signal $\sim 200\mu s$ which is called “delayed signal”, 2.2 MeV gamma-ray (An et al., 2016). Both signals are excellent to extract from other BG signal. However, IBD is better for low neutrino energy $E_{\nu_e} \lesssim 60$ MeV (Vogel and Beacom, 1999). The most signal which hit nuclei in LS is a prompt photon that is difficult to indicate the source. Nonetheless, the spectrum profile, energy range, and pulse shape can be distinguished the signal from BG signal.

2.4 JUNO detector and JUNO software framework

The JUNO experiment can receive the neutrinos from most of the directions which allow us to study the source of neutrino from WIMPs annihilation. We use JUNO software framework to predict this event when it strikes material in a detector. This section reports the location and components of JUNO experiment in section 2.4.1 and software framework in section 2.4.2.

2.4.1 JUNO detector

The JUNO is under-constructed neutrino experiment and has multipurpose to study neutrinos such as to determine neutrino mass hierarchy, precisely measure oscillation parameters, detect astrophysical and geological neutrinos. However, the primary purpose is to study mass hierarchy from antineutrino from a nuclear reactor. This reason is why the detector position is close to Nuclear Power Plant (NPP). The location is Jiangmen city in Guangdong province in China away from Yangjian and Taishan NPP around 53 km (An et al., 2016) with longitude $112^{\circ}31'05''$ and north latitude $22^{\circ}07'05''$. The JUNO is under the granite mountain that is suitably reduced cosmic ray. Its detector consists of three main parts: the Central Detector (CD), VETO and shield, and muon tracker as shown in Figure 2.6 (Wurm, 2017). The CD is an important part of neutrino detector. It comprises the LS detector with 20 kiloton and has diameter 35.4 km. The outside CD sphere surrounds with the PMTs to detect the photon from neutrino interaction with the LS. The VETO and shield consist of a pure water tank to protect from other radioactivity and PMTs to detect Cherenkov light, indicating cosmic ray event. On top of the tank, the muon tracker is installed to measure muon direction and have functioned as VETO.

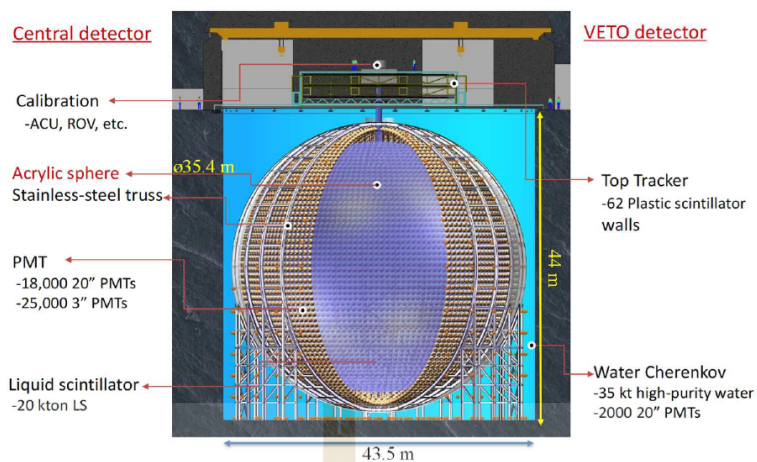


Figure 2.6 Schematic view of JUNO detector (Wurm, 2017).

2.4.2 JUNO software framework

The JUNO software framework is Monte–Carlo (MC) simulation to predict detector simulation of the neutrino by JUNO experiment. The offline data processing of JUNO is developed based on SNI–PER (Software for Non–collider Physics ExperRiment) framework. It consists of physics generators, detector simulation, electronic simulation, reconstruction modules as shown in Figure 2.7. The MC simulation software has played an important role in optimizing detector parameter and studying physics in physics generator.

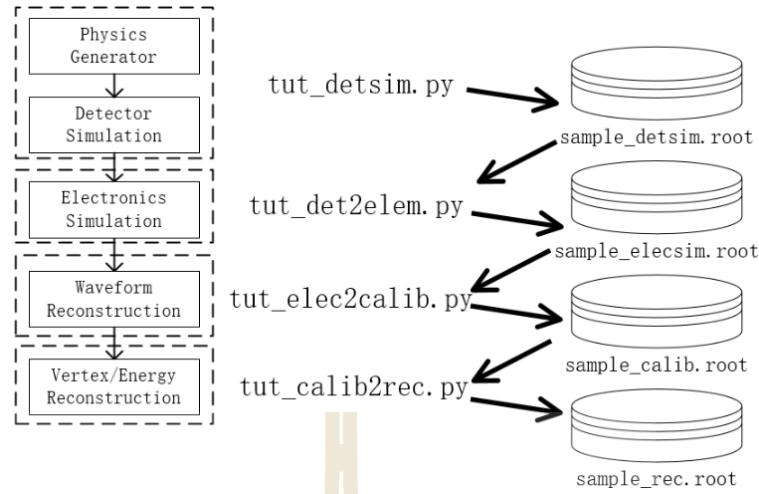


Figure 2.7 Offline Processing Full Chain (Lin, 2016).

The physics generators depend on the source of neutrino signals such as solar neutrino, SuperNova (SN) neutrino, and atmospheric neutrino. Their functions are that generate neutrino spectrum (their energy and momentum) and most of them based on MC. The detector simulation uses Geant4 as MC which include the effect of properties, type, number and position of PMTs, and JUNO geometry. The result from detector simulation display how the detector obtains the photon from the neutrino interacting with LS. The physics generator integrates with detector simulation on interface code: `tut_detsim.py` for JUNO software framework as displayed in Figure 2.7. The electronic simulation account electronic equipment impact such as electronic dark noise and electronic readout. The calibration is waveform reconstruction from muon track and photon hit. The final process is vertex reconstruction to estimate visible neutrino energy after neutrino strike nuclei in LS. In this work, we emphasize only `tut_detsim.py` and its component as Figure 2.8. The physics generator simulates neutrino spectrum and calculates the neutrino interaction with LS by providing the outcoming particle energy and 3–momentum. It is required an algorithm to connect between physics generator and detector simulation.

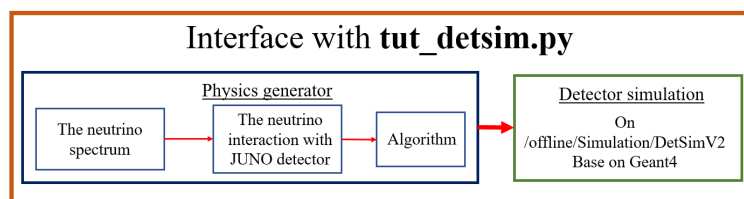
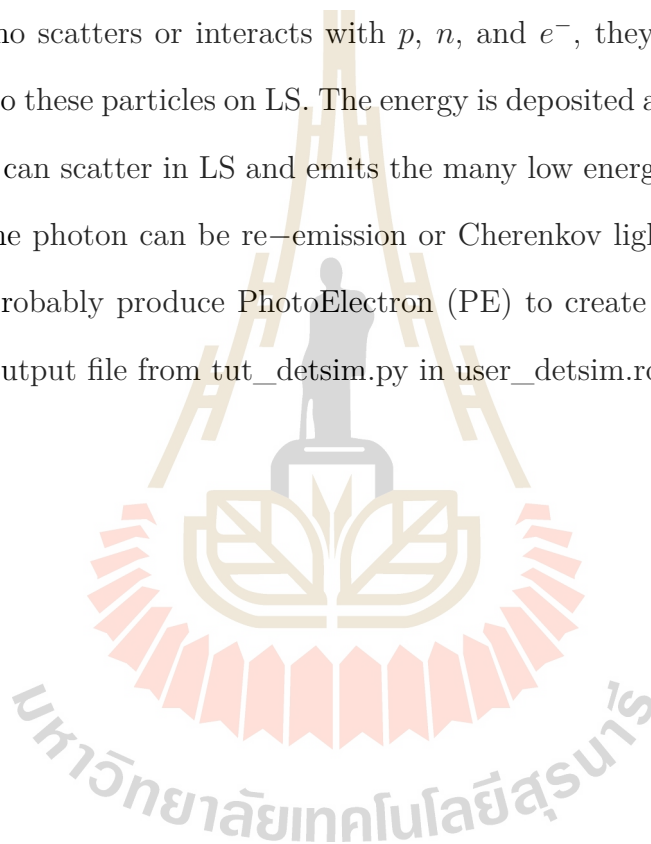


Figure 2.8 Offline Processing inside `tut_detsim.py`.

The process to detect neutrino signal on detector simulation is described: when neutrino scatters or interacts with p , n , and e^- , they transfer energy and momentum to these particles on LS. The energy is deposited and emits the photon. This photon can scatter in LS and emits the many low energetic photons: optical photon. Some photon can be re-emission or Cherenkov light. These photon hit PMTs and probably produce PhotoElectron (PE) to create the signal. We have to store an output file from `tut_detsim.py` in `user_detsim.root` for analysis.



CHAPTER III

METHODOLOGY

The aim of this work is to simulate the neutrino signal from captured WIMPs annihilation inside the sun's core. Nevertheless, the JUNO experiment has a low energy threshold which could detect low energetic neutrino from low mass of WIMPs annihilation in GC. Therefore, we would like to calculate the neutrino event rate from WIMPs annihilation coming from GC and the Sun's core in section 3.1 and integrated neutrino spectrum on the offline framework in section 3.2.

3.1 Calculation of neutrino event rate from WIMPs annihilation

The neutrino can be produced by WIMPs self-annihilation. Consequently, neutrino detector on the Earth can obtain this signal.

3.1.1 WIMPs annihilation into neutrinos in the Milky Way galaxy

The different flux of neutrino and antineutrino flux per flavor directly from WIMPs annihilation ($\chi\chi \rightarrow \nu\bar{\nu}$) from the MW halo is (Palomares-Ruiz and Pascoli, 2008)

$$\frac{d\Phi}{dE_\nu} = \frac{\langle\sigma v\rangle_{\chi\chi}}{2} J_{avg} \frac{R_{sc}\rho_0^2}{m_\chi^2} \frac{1}{3} \delta(E_\nu - m_\chi) \quad (3.1)$$

where m_χ is the WIMPs mass and $\langle\sigma_{A\nu}\rangle$ is WIMPs self-annihilation cross section in equation (2.2). The factor $1/2$ refers anti-WIMPs which mean that anti-WIMPs is its own WIMPs, and the factor of $1/3$ comes from the average branching ratio of annihilation to three neutrino flavors owing to neutrino oscillation. Consequently, the neutrino spectrum is provided by delta function which determines the WIMPs annihilation transferring energy and produce neutrino directly. The J_{avg} is an average J-factor and use the canonical value equal to 5 in order to get rid of divergent calculation. The R_{sc} is a distance from GC to sun which is 8.5 kpc and ρ_0 is local WIMPs density as in Table 3.1. The number of neutrino event on the detector is as (Palomares-Ruiz and Pascoli, 2008)

$$N \simeq \sigma_{det}(m_\chi)\Phi N_{target}t\epsilon \quad (3.2)$$

where σ_{det} is cross-section detector to receive neutrino signal with $E_\nu = m_\chi$, Φ is total neutrino or antineutrinos flux, N_{target} is the number of target particles in a detector, t is the time-exposure, and ϵ is the detector efficiency that depends on neutrino interaction with N_{target} . The equation (3.1) represents the higher mass reduces the differential flux by square WIMPs mass. We consider low WIMP mass from 20 MeV to 60 MeV because neutrino energy less than 20 MeV is hard to separate the signal from the solar neutrino and reactor neutrino events. We determine IBD cross-section in equation (3.3) as described in Vogel and Beacom (1999), N_{target} is proton on JUNO 1.45×10^{33} and JUNO's efficiency for IBD is 73% (An et al., 2016).

$$\sigma_{IBD} = 0.0952 \left(\frac{E_e^0 p_e^0}{1MeV^2} \right) \times 10^{-42} \quad cm^2 \quad (3.3)$$

where E_e^0 is positron energy which compute as $E_e^0 = E_\nu - (M_n - M_p)$ with a mass of neutron (M_n) and proton (M_p) in MeV and p_e^0 is the positron momentum which

evaluates as $p_e^0 = \sqrt{(E_e^0)^2 - m_e^2}$ with a mass of electron m_e .

3.1.2 Solar captured WIMPs annihilation inside the Sun's core

The differential neutrino flux from solar captured WIMPs annihilation ($\chi\chi \rightarrow f\bar{f}$) can be computed by An et al. (2016)

$$\frac{d\Phi_{\nu\beta}^{\chi\chi}}{dE_\nu} = P_{\nu_\alpha \rightarrow \nu_\beta}(E_\nu, D) \frac{\Gamma_A}{4\pi D^2} \Sigma_f B_\chi^f \frac{dN_{\nu_\alpha}^f}{dE_\nu} \quad (3.4)$$

where $P_{\nu_\alpha \rightarrow \nu_\beta}(E_\nu, D)$ is the neutrino oscillation probability from the source to the detector which is calculated using equation (2.8), Γ_A is the DM annihilation rate, B_χ^f is the branching ratio for the DM annihilation channel ($\chi\chi \rightarrow f\bar{f}$) such as $\tau\bar{\tau}$, $\nu\bar{\nu}$ and $b\bar{b}$, D is the distance between the source and detector, and $\frac{dN_{\nu_\alpha}^f}{dE_\nu}$ is defined as the energy spectrum of ν_α (for $\alpha = e, \mu, \tau$).

The annihilation rate (Γ_A) depends on the number of WIMPs in the Sun's core which is evolved with time since the Sun formed in the below equation (An et al., 2016).

$$\frac{dN}{dt} = C_c - C_a N^2 - C_e N \quad (3.5)$$

where C_c is the capture rate, $C_a N^2$ is the annihilation rate, and $C_e N$ is the evaporation rate. The total annihilation event in the solar core is $\frac{C_a N^2}{2}$ where 1/2 is the anti-WIMPs for self-annihilation. The WIMPs masses below 3 to 4 GeV may evaporate from the Sun hence evaporation of WIMPs in the mass range 10–1,000 GeV can be ignored (An et al., 2016). Thereby, the equation is reduced to

$$\frac{dN}{dt} = C_c - C_a N^2 \quad (3.6)$$

The number of WIMPs at this time can be found by

$$N = \sqrt{C_c C_a} \tanh(\sqrt{C_a C_c} t + \text{constant}) \quad (3.7)$$

For initial condition at $t = 0$, $N = 0$ hence

$$N = \sqrt{\frac{C_c}{C_a}} \arctan(\sqrt{C_a C_c} t) \quad (3.8)$$

Thus, the number of WIMPs at present ($t_{\odot} = 4.603 \times 10^9$ years) is $N = \sqrt{\frac{C_c}{C_a}}$, where C_a is annihilation factor which can be estimated from (Jungman et al., 1996)

$$C_a \simeq 5.16 \times 10^{-57} \left(\frac{m_{\chi}}{\text{GeV}}\right)^{3/2} s^{-1} \quad (3.9)$$

For long time collected number of WIMPs, we can assume the equilibrium between capture rate and annihilation rate using the equation (3.10). The captured rate consider spin of material inside the sun: Spin-Independent (SI) or scalar and Spin-Dependent (SD) or axial vector interaction more detail to compute it see Jungman et al. (1995).

$$\Gamma_A = \frac{C_c}{2} \quad (3.10)$$

The effect of SD cross section at the sun is stronger than SI (Wechakama, 2013). In this thesis, we focus on SD interaction and WIMPs - hydrogen elastic scattering cross-section ($\sigma_{SD}^{\chi-H}$) which assume to equal WIMPs-proton elastic scattering cross section ($\sigma_{SD}^{\chi-p}$). The approximate capture rate for SD interaction (C_{SD}) of WIMPs and dominated atom, hydrogen in the Sun is given by (Edsjo et al., 2018)

$$C_{SD} = (1.3 \times 10^{23} s^{-1}) \left(\frac{270 \text{ km s}^{-1}}{\bar{v}}\right) \left(\frac{\rho_0}{0.3 \text{ GeV cm}^{-3}}\right) \left(\frac{100 \text{ GeV}}{m_{\chi}}\right) \left(\frac{\sigma_{SD}^{\chi-p}}{10^{-40} \text{ cm}^2}\right) \quad (3.11)$$

where ρ_0 is local WIMPs density and \bar{v} is WIMPs velocity dispersion which is computed by viral theorem $\bar{v} \simeq \sqrt{\frac{GM_\chi}{R_\odot}}$ with M_χ is a total mass of WIMPs in GC to the Sun and R_\odot is a distance of the Sun from GC. Both of them depend on WIMPs density profile in equation (2.3), (2.4), and (2.5) and using fitted parameters in Table 2.1 and their values are shown in Table 3.1. and m_χ represent a mass of WIMPs. The NFW profile provided the high total WIMPs mass thus the velocity dispersion is higher than the other. The International Astronomical Union (IAU) agreement of rotation velocity at the Sun's distance from GC (v_0) is 220 km/s thus velocity dispersion is from $\bar{v} = \sqrt{\frac{3}{2}}v_0 = 270$ km/s (Jungman et al., 1996). For the dark matter density model and relative the radius with circular rotation speed present that the local dark matter density is $0.3 \text{ GeV}/\text{cm}^{-3}$ (Jungman et al., 1996). Therefore, the fiducial model reports $\rho_0 = 0.3 \text{ GeV}/\text{cm}^3$ and $\bar{v} = 270$ km/s.

Table 3.1 The local WIMPs density and velocity dispersion (Nesti and Salucci, 2013).

WIMP density profile	Local density (GeV/cm^3)	Velocity dispersion (km/s)
NFW	0.43	170.67
Einasto	0.30	144.23
Burkert	0.44	149.46

The annihilation rate in equation (3.10) is shown in Figure 3.1 as a function of WIMPs mass. The annihilation rate is reduced by massive WIMPs mass due to the less number density. The different MW DM halo profiles give slightly different capture rate because of their local density and WIMPs velocity dispersion.

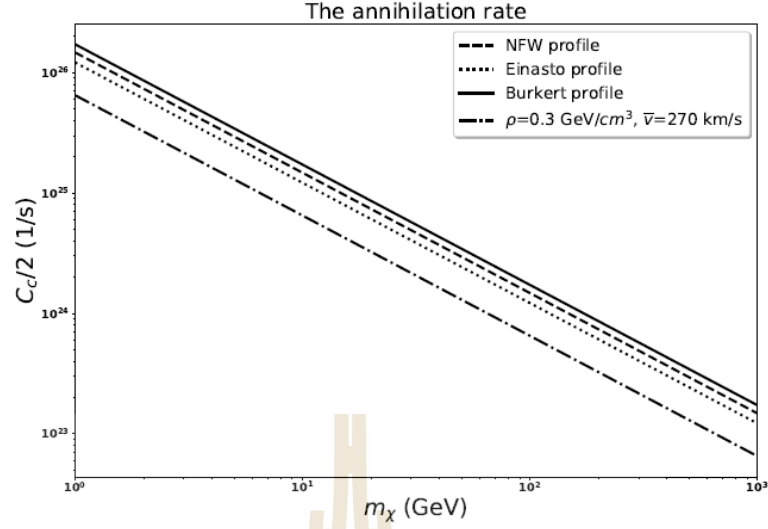


Figure 3.1 The annihilation rate with different MW DM halo profile which gives the different value of local density and dispersed velocity and using the $\sigma_{\chi p}^{SD} = 10^{-39} \text{cm}^2$. The dashed line uses NFW profile. The dotted line uses Einasto profile. The solid line uses Burkert profile. The dotted–dashed line is the fiducial model with $\rho_0 = 0.3 \text{ GeV}/\text{cm}^3$ and $\bar{v} = 270 \text{ km/s}$.

The WimpSim package is simulated neutrino energy spectrum (dN/dE) with WIMPs mass range in GeV which we selected WIMPs mass equal to 10, 100, and 1,000 GeV for the different profile by different order magnitude of WIMPs mass. We set an annihilation rate of 2.5×10^6 . Examples of neutrino spectra which are simulated using the WimpSim package are shown in Figure 2.5 and Figure 2.6 for WIMPs mass 10 GeV and 1,000 GeV, respectively.

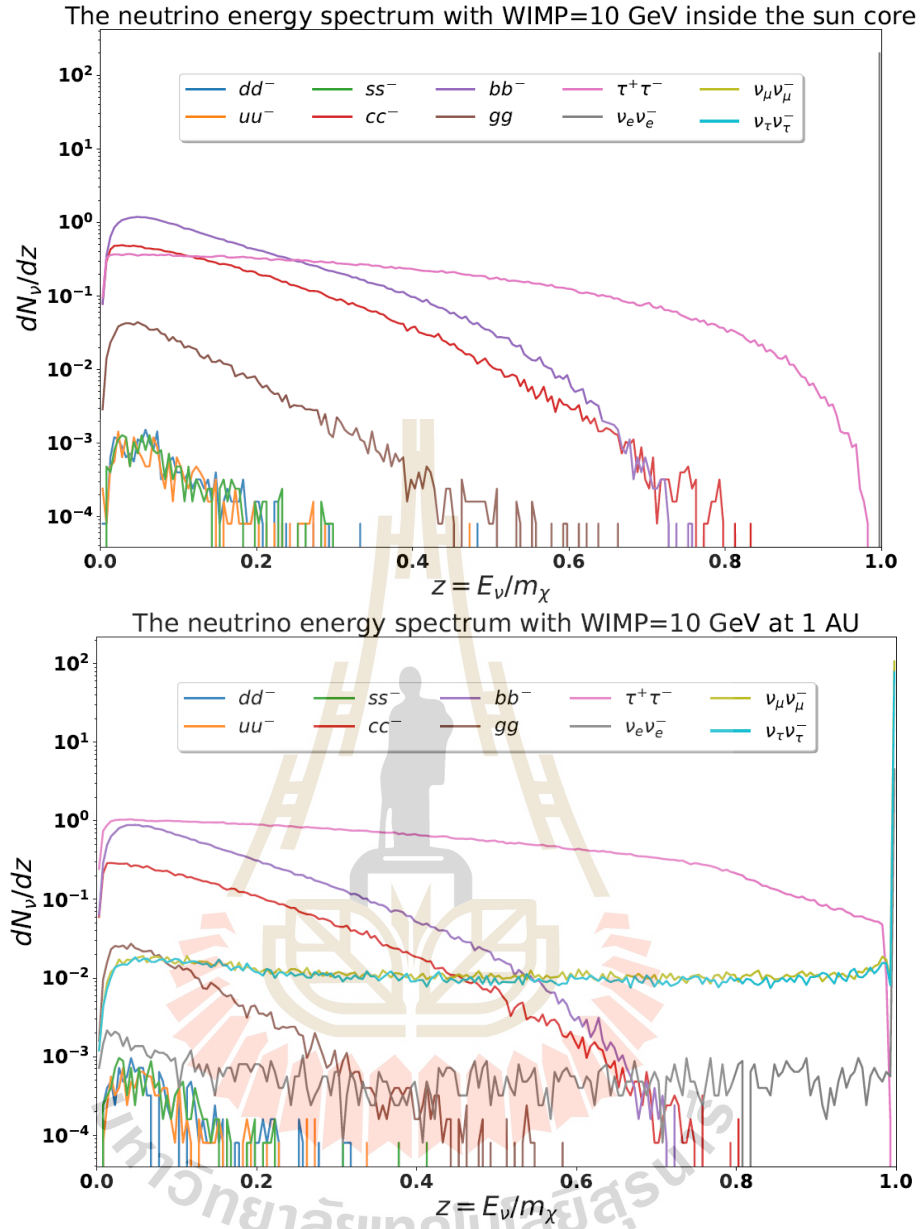


Figure 3.2 The electron neutrino spectrum with the ratio of neutrino energy (E_ν) and mass of WIMPs (m_χ) by using 10 GeV in the Sun's core for an upper figure and 1 AU for a lower figure. Each of the color lines is different particle channels from DM annihilation.

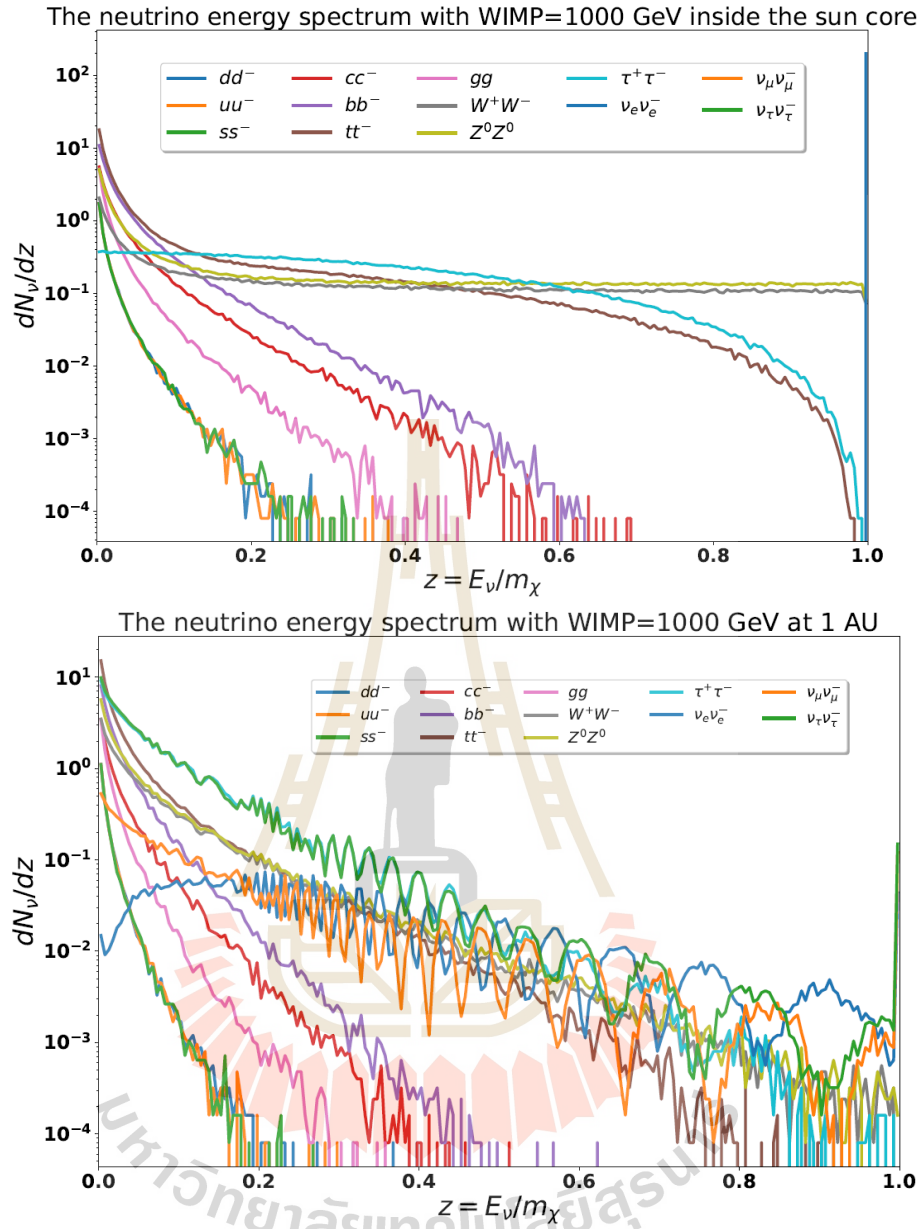


Figure 3.3 The electron neutrino spectrum with the ratio of neutrino energy (E_ν) and mass of WIMPs (m_χ) by using 1 TeV in the Sun's core for an upper figure and 1 AU for a lower figure. Each of the color lines is different particle channels from DM annihilation.

When WIMPs mass is higher, it can generate more energetic channels such as $t\bar{t}$, W^+W^- , and Z^0Z^0 . The $\tau^-\tau^+$ is a dominant annihilation channel. At the solar core, the neutrino channel is raised up by direct WIMPs annihilation like

in section 3.1.1. and for 1 AU, the three flavor neutrino increase from tau decay that is produced in Charge Current (CC) interaction by tau neutrinos annihilated channel. Both of distances show neutrino oscillation in the spectrum arising out the Earth. The position, WIMPs mass, and annihilated channel give different spectral profile.

We consider the two dominate annihilation channels which are $\tau^-\tau^+$ and $\nu_\tau\bar{\nu}_\tau$. The branching ratio for each channel equals to 1 ($B_x^{\tau,\nu_\tau} = 1$) for the simplify model to calculate the differential neutrino flux in equation (3.4). The electron neutrino energy spectrum (dN/dE) by WimpSim package is in summary file on line 13 for 1 AU. The neutrino event rate in the detector reads as (An et al., 2016)

$$N = \int_{E_{th}}^{m_\chi} \frac{d\Phi_\nu^{xx}}{dE_\nu} A(E_\nu) dE_\nu d\Omega \quad (3.12)$$

where E_{th} is the detector's threshold energy and $A(E_\nu)$ is the detector's effective area which depends on type of LS, neutrino energy and electronic devices. It is calculated by equation (3.13). Ω is the solid angle of the event which is related to the half angle of the observation cone of a detector by $2\pi(1 - \cos\Phi)$ where $\Phi = 30^\circ$ according collection efficiency (An et al., 2016). The JUNO's effective is given by (An et al., 2016)

$$A(E_\nu) = [n_p\sigma_{\nu p} + n_n\sigma_{\nu n}]\epsilon(E_\nu) \quad (3.13)$$

where n_p and n_n are proton and neutron number on JUNO experiment, respectively. $\sigma_{\nu p}$ and $\sigma_{\nu n}$ are neutrino–proton and neutrino–neutron scattering interaction on JUNO's LS, respectively. We use the fitting value on Table 3.2 and simplify the total cross–section in equation (3.14) to apply neutrino–nucleon in JUNO detector (Edsjo, 2007). The energy–dependent efficiency ($\epsilon(E_\nu)$) is less than 1% for E_ν 1 GeV and it is greater than 70% for $E_\nu > 5$ GeV (An et al., 2016).

In the WimpSim package, the neutrino interaction with other particles such as protons (p) and neutrons (n) inside the sun and using **nusigma** code (Edsjo and Niblaeu, 2017) to calculate the neutrino propagate from the solar core to the solar surface. From the program, it considers which neutrino scattering off proton and neutron as target and assumes isospin symmetry, and also calculates the total neutrino cross-section by using Parton Distribution Functions (PDFs) to integrate differential cross-section with a fraction of momentum transfer and energy (Edsjo, 2007). For saving time running of the program, it interpolates table in **nusigint** code to calculating cross-section. For WIMPs mass in the range of $10-10^4$ GeV, parameters will be fitted with different neutrino interaction as CC and NC in Table 3.2 and using simplify an equation to calculate the total interaction cross-section in equation (3.14).

Table 3.2 The fitted parameters of the neutrino–nucleon cross-sections.

Interaction	a [pb = $10^{-40} m^2$]	b
CC $\nu \rightarrow p$	5.43×10^{-3}	0.965
CC $\bar{\nu} \rightarrow p$	4.59×10^{-3}	0.978
CC $\nu \rightarrow n$	1.23×10^{-3}	0.929
CC $\bar{\nu} \rightarrow n$	2.19×10^{-3}	1.022
NC $\nu \rightarrow p$	2.48×10^{-3}	0.953
NC $\bar{\nu} \rightarrow p$	1.22×10^{-3}	0.989
NC $\nu \rightarrow n$	2.83×10^{-3}	0.948
NC $\bar{\nu} \rightarrow n$	1.23×10^{-3}	0.989

$$\sigma = a\left(\frac{E_\nu}{\text{GeV}}\right)^b \quad (3.14)$$

The Table 3.2 and equation (3.15) provide error less than 10% from full calculation but for lower 10 GeV and higher 10^4 GeV are overestimated which display in Figure 3.4.

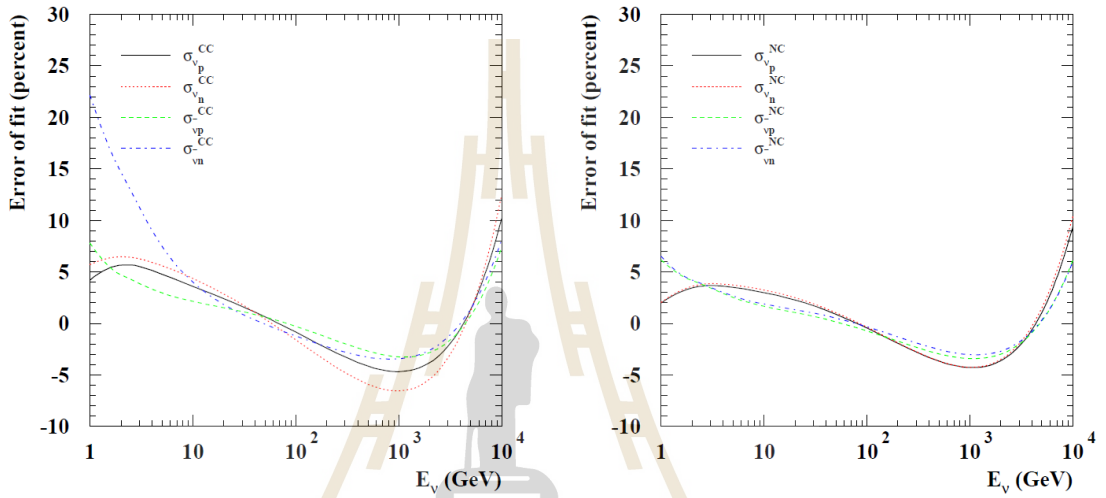


Figure 3.4 The error of the parameterizations (in %) of the total cross-sections with different interaction as a function of neutrino energies in GeV (Edsjo, 2007).

In Figure 3.5 illustrates the total neutrino scattering cross-section with proton and neutron via CC and NC interaction as a function of neutrino energy by using equation (3.14) and fitting parameters in Table 3.2. The large neutrino energy obtain the high value of cross-section and neutrino-neutron scattering via NC is influenced than the other.

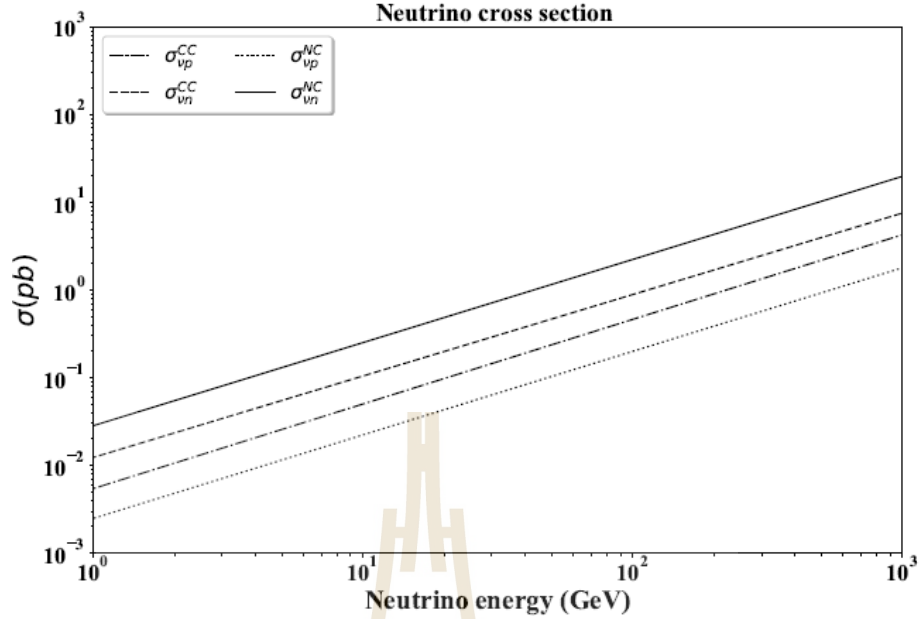


Figure 3.5 The total cross-section as a function neutrino energy in GeV. The dotted-dashed line is a total neutrino-proton cross-section via CC. The dotted line is a total neutrino-proton cross-section via NC. The dashed line is a total neutrino-neutron cross-section via CC. The solid line is a total neutrino-neutron cross-section via NC.

3.2 Neutrino from solar captured WIMP annihilation on detector simulation

We use the neutrino spectrum from WimpSim package for physics generator on offline framework version J17v1r1. Firstly, the WimAnn is using to simulate the neutrino spectrum and this program requires input parameter: WIMPs mass, oscillation parameters which use following JUNO Yellowbook (An et al., 2016), number of annihilation equals to 2.5 million events, and $\tau^-\tau^+$, $\nu\bar{\nu}_\tau$ annihilation channel. We set the mass of WIMPs: 10, 100, and 1,000 GeV as same as the previous section. Next, we insert an event file from each annihilation channel

in WimpEvent for certain location of JUNO experiment. The output file from WimpEvent shows detail neutrino flavor incoming to a detector and the particle outcoming after colliding targets. We select the neutrino flavor: electron neutrino and incoming neutrino energy for calculated our interaction with LS.

We integrate these neutrino energies in solar neutrino generator by adding more channel on it (-type DM). The workflow of a solar neutrino is in Figure 3.6.

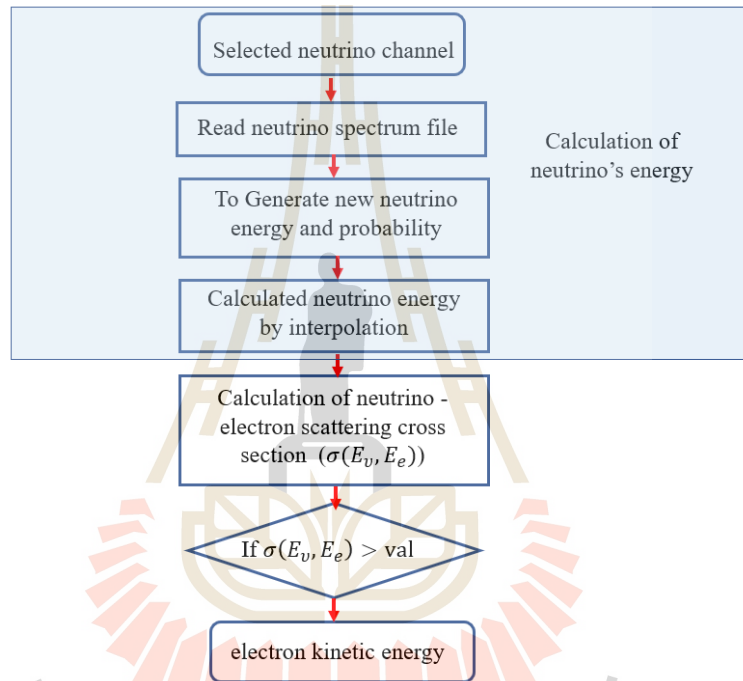


Figure 3.6 The scheme of solar neutrino generator. The $\text{val} = \text{UniformRand}()$ and $\sigma(E_\nu, E_e)$ is a normalized cross-section.

Firstly, we have to calculate neutrino energy by inputting the neutrino spectrum. There are neutrino energy and probability. We set our spectrum file following a solar neutrino spectrum file by using the histogram module in Python to set a range of neutrino energy and a number of neutrino for each range. For our probability is that neutrino number in each range energy divide total numbers of neutrino. Next, It sets new neutrino energy range for consistent calculation of electron energy in before lasted process and uses cumulative distribution to

find probability of this neutrino energy following input neutrino spectra file. The interpolation uses to compute neutrino energy in equation (3.15)

$$y = \frac{\Delta y}{\Delta x}(x - x_0) + y_0 \quad (3.15)$$

where y represents neutrino energy, y_0 represents lower neutrino energy in a range x as x is a probability which is random number (0.–1.) by **UniformRand()** according to uniform distribution and x_0 is probability for neutrino energy (y_0).

After it obtained a neutrino energy, it evaluates the normalized $\nu - e$ cross-section that gives the value between 0.–1. by dividing the cross-section for each neutrino energy and electron energy with the maximum cross-section. The final process is to generate kinetic electron energy to verify the normalize cross-section with probability of interaction by **UniformRand()**.

The electron energy is used in Geant4 on detector simulation to compute their 4-momentum in LS and simulate a number of PE, their hit time (hit-Time) and pulse shape in PMTs and deposited energy (edep). We use the results from detector simulation of solar neutrino and the atmospheric neutrino to compare with neutrino from solar captured WIMPs annihilation inside core of the Sun. The channel Be8 of solar neutrino is dominated channel for neutrino from thermonuclear fusion in the Sun and particular $\nu - e^-$ scattering interaction. The atmospheric neutrino spectrum is generated by GENIE (An et al., 2016) and input spectrum file for `tut_detsim.py` from the directory: `$JUNO-TOP/data/Generator/NuAtm/data/tree_100000100.root`. The input file stores atmospheric neutrino energy, x, y, z momentum and etc. The `tut_detsim.py` needs to input neutrino event by command `--evtmax` and we define 1,000 events for distribution to analyze data and deduction time to running offline.

CHAPTER IV

RESULT AND DISCUSSION

This chapter is explained the calculation of neutrino events resulting from WIMPs annihilation from GC and captured WIMPs in the center of Sun and shows an integrated JUNO detector simulation.

4.1 Result of neutrino event rate from WIMPs annihilation

The number of neutrino event rate from WIMPs annihilation is anticipated to distinguish from the other neutrino BG events on a detector in duration.

4.1.1 The neutrino flux from WIMPs annihilation in the Milky Way galaxy

The differential neutrino flux depends on WIMPs mass and WIMPs density profiles for local DM density. We plot the differential neutrino flux with various WIMPs mass and use Burkert profile due to the largest local DM density in Figure 4.1.

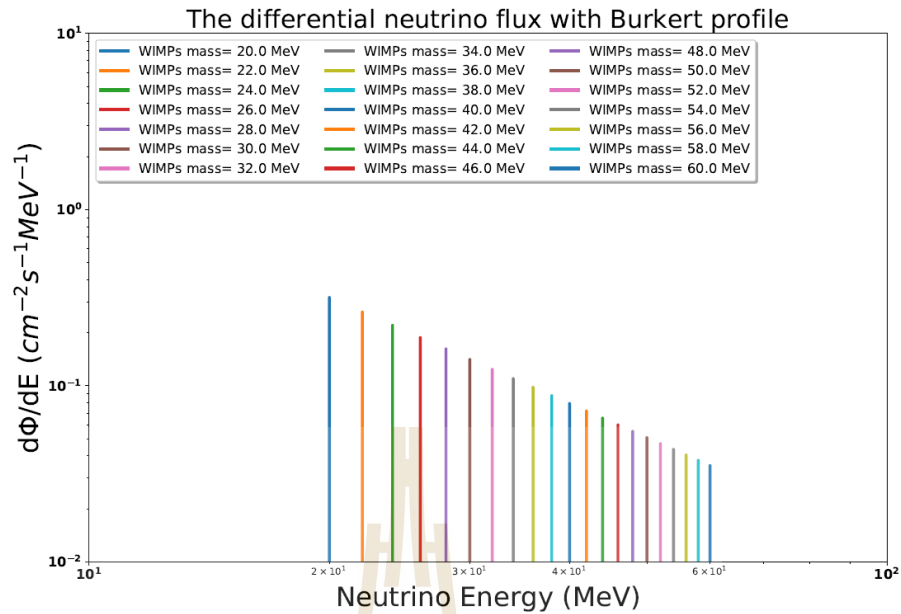


Figure 4.1 The differential neutrino flux from GC with Burkert profile and each color lines presents WIMPs mass between 20 MeV to 60 MeV.

The differential neutrino flux is decreasing dramatically by heavy mass and the shape of the graph is given by delta function which represents direct neutrino spectrum from WIMPs self-annihilation without losing energy to an environment. The detector can only receive the neutrino event. Thereby, the number of neutrino events from WIMPs per neutrino energy is displayed in Figure 4.2 for 10 years of JUNO talking data.

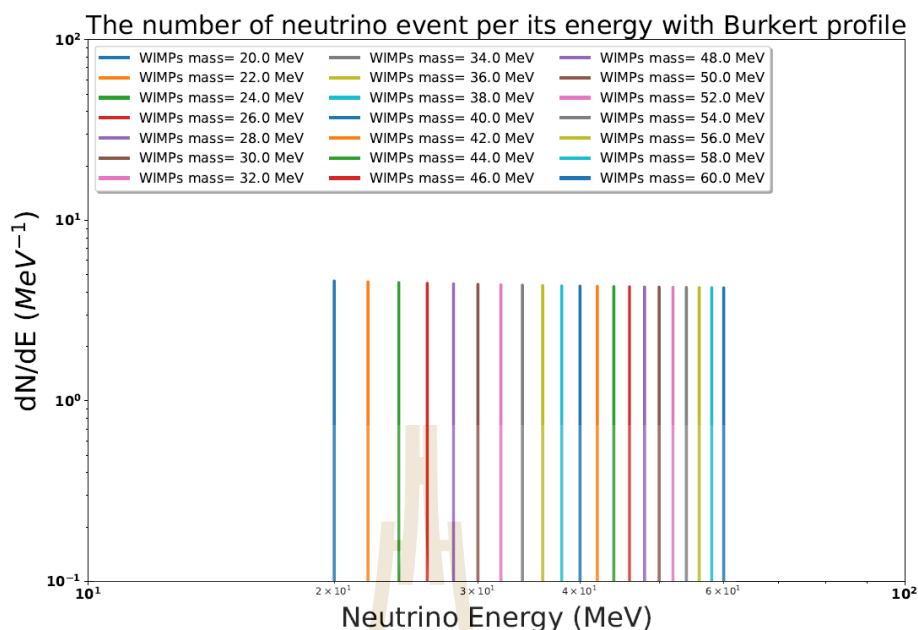


Figure 4.2 The number of neutrino per neutrino energy (dN/dE) using Burkert profile, WIMPs mass in a range 20 MeV–60 MeV, IBD cross-section and time exposure 10 years

The cross-section affects to dN/dE in Figure 4.1 to provide rather same amplitude for this WIMPs mass range. The number of events of these neutrinos on JUNO is approximately 4 events per 10 years for 20 MeV. The number of events is very low and hard to distinguish neutrino event from BG sources such as atmospheric neutrinos.

4.1.2 The neutrino flux from captured WIMPs annihilation inside the Sun's core

The neutrino can be also produced directly or finally decay from the production of captured WIMPs annihilation inside the Sun's core. In Figure 4.3 demonstrates the neutrino events per its energy from solar captured WIMPs self-annihilation in WIMPs mass range GeV on JUNO experiment.

We use the electron neutrino spectrum (dN/dE) from WimpSim package to estimate the neutrino events per 1 year on JUNO experiment for WIMPs mass equal to 10, 100, and 1,000 GeV as Figure 4.3, 4.4, and 4.5, respectively. For $\tau^-\tau^+$ channel, the neutrino events on JUNO detector are 12, 5, 2 events for WIMPs mass equal to 10, 100, 1,000 GeV, respectively. For $\nu_\tau\bar{\nu}_\tau$ channel, the neutrino events on JUNO detector are 29, 3, 2 events using WIMPs mass 10, 100, 1,000 GeV, respectively. The neutrino events from captured WIMPs annihilation inside the Sun's core decrease with heavy WIMPs mass and is related to the neutrino spectrum especially the annihilated neutrino channel. The energy spectrum from tau neutrino channel is jumping at the neutrino energy closed to the mass of WIMPs due to the direct annihilated channel and provide the more neutrino events than $\tau^-\tau^+$ channel which is clearly displayed in the light mass of WIMPs as Figure 4.3.

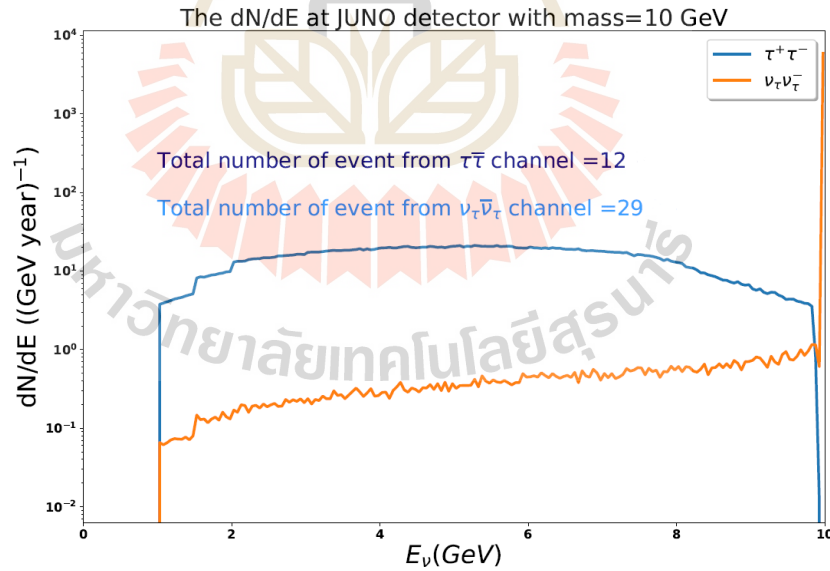


Figure 4.3 The number of electron neutrinos per its energy (dN/dE) with WIMPs mass 10 GeV, consider neutrino–nucleon scattering cross–section and integration time 1 year. The blue line is from $\tau^-\tau^+$ channel and the orange line is from $\nu_\tau\bar{\nu}_\tau$ channel.

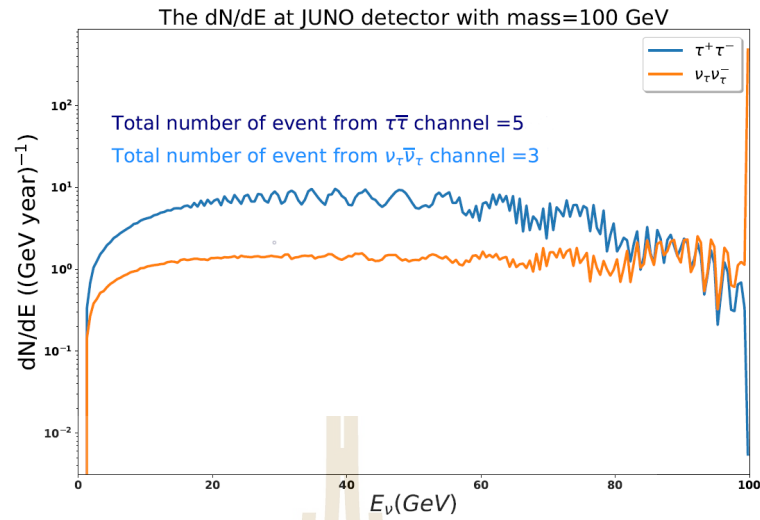


Figure 4.4 The number of electron neutrinos per its energy (dN/dE) with WIMPs mass 100 GeV, consider neutrino–nucleon scattering cross–section and integration time 1 year. The blue line is from $\tau^-\tau^+$ channel and the orange line is from $\nu_\tau\bar{\nu}_\tau$ channel.

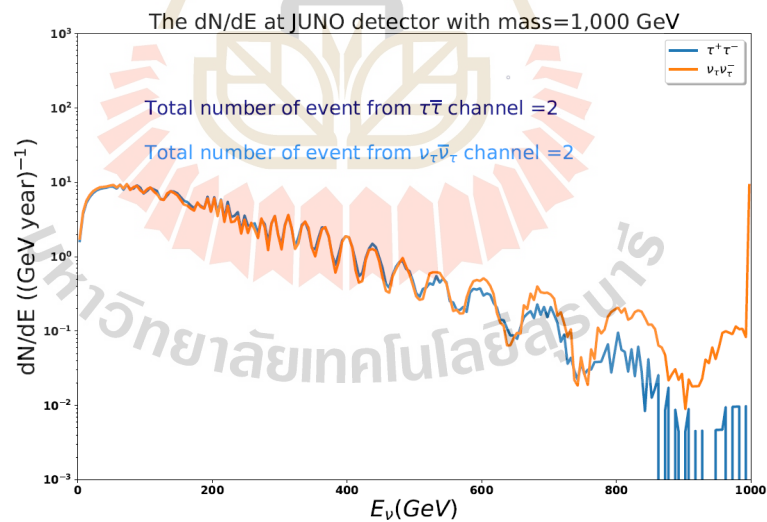


Figure 4.5 The number of electron neutrinos per its energy (dN/dE) with WIMPs mass 1,000 GeV, consider neutrino–nucleon scattering cross–section and integration time 1 year. The blue line is from $\tau^-\tau^+$ channel and the orange line is from $\nu_\tau\bar{\nu}_\tau$ channel.

We use the local density and dispersion velocity following the fiducial model and give the WIMPs–proton cross–section equal to $1 \times 10^{-39} \text{ cm}^2$ following An et al. (2016). The $\sigma_{\chi p}^{SD}$ is a major variable to calculate the number of events. It is lessened by lower $\sigma_{\chi p}^{SD}$ as a function of annihilation rate. There are many parameters and operators to calculate WIMPs–proton cross–section and at present, the sensitivity of detector for direct WIMPs search is lower limited of $\sigma_{\chi p}^{SD}$ to $2 \times 10^{-41} \text{ cm}^2$ for WIMPs mass 25 GeV but there are not still confirm WIMPs signal (Amole et al., 2019).

4.2 Result of neutrino from solar captured WIMPs annihilation on detector simulation

We have integrated all neutrino spectrum from dominate channel: $\tau\bar{\tau}$. It has been simulated by WimpSim package on detector simulation to compare and analyze with the solar neutrino and the atmospheric neutrino. The number of neutrino events on detector simulation is 1,000 events. The output file from detector simulation provides the histogram of totalPE that is the number of PE for each event, hitTime which is a hit time of PE in PMTs, edep that is energy deposition after neutrino collides LS, and etc. These data are used in vertex reconstruction method to determine the exact location of the neutrino interacting with LS particles. However, this thesis demonstrates only result from detector simulation. Firstly, we compare the total number of PE between electron neutrino (ν_e) and tau and muon neutrino (ν_x) from captured WIMPs mass equal to 10 GeV and $\tau^-\tau^+$ annihilated channels in Figure 4.6.

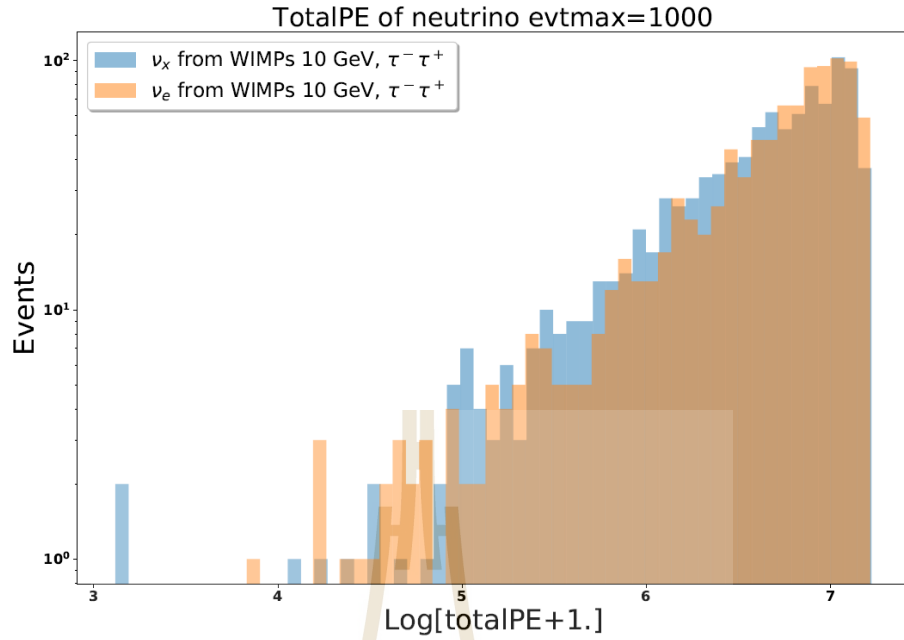


Figure 4.6 The histogram of the total number of PE from capture WIMPs mass equal to 10 GeV and $\tau^- \tau^+$ annihilated channels with blue histogram is ν_x and orange histogram is ν_e .

Most of the neutrino events allow a lot of total number of PE. The distribution of this histogram for neutrino flavor is similar to each other but JUNO experiment is sensitivity for an electron neutrino. Therefore the further results from solar captured WIMPs are focus only electron neutrino.

In Figure 4.7, 4.8, and 4.9 display the total number of PE for neutrino events on detector simulation from solar captured WIMPs mass equal to 10 GeV, atmospheric neutrino, and solar neutrino, respectively. We would like to compare histogram of the total number of PE from three sources as mention earlier in Figure 4.10.

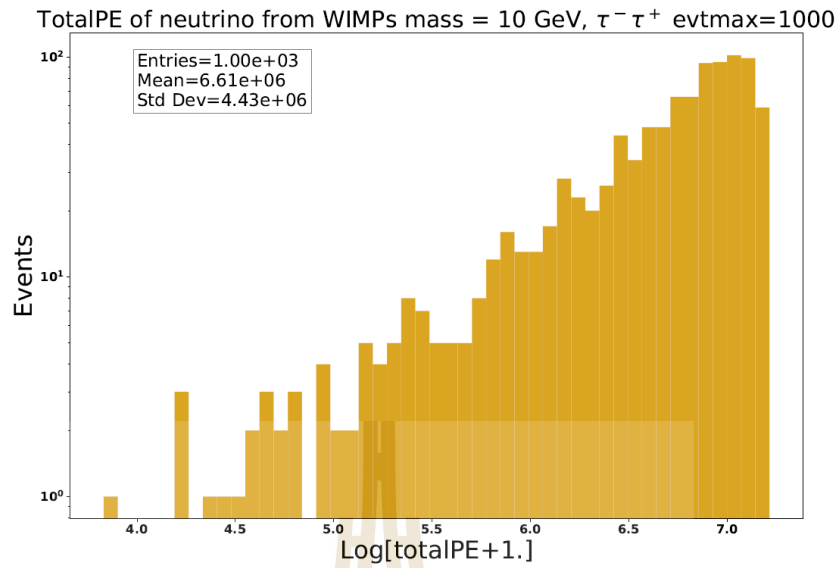


Figure 4.7 The histogram of the total number of PE from captured WIMPs mass equal to 10 GeV. The mean of PE numbers is 6.61×10^6 and the standard deviation of this plot is 4.43×10^6

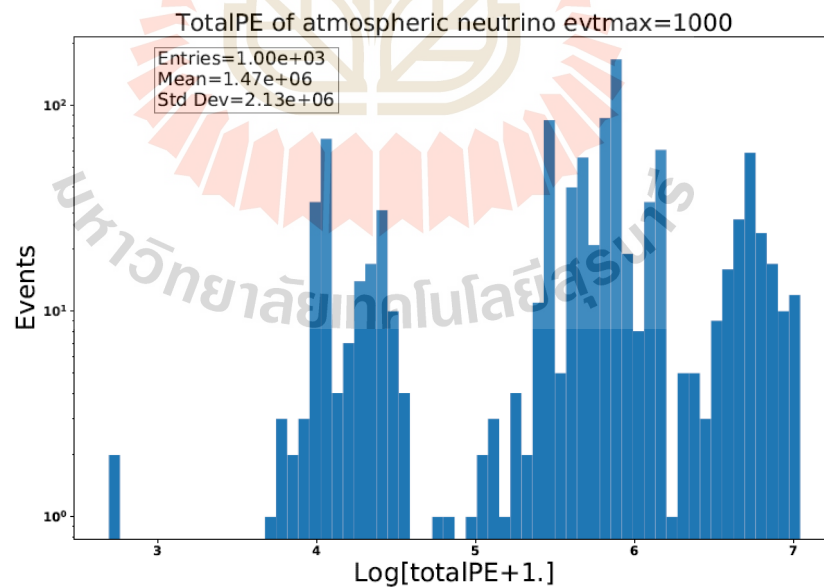


Figure 4.8 The histogram of the total number of PE from atmospheric neutrino. The mean of PE numbers is 1.47×10^6 and the standard deviation of this plot is 2.13×10^6

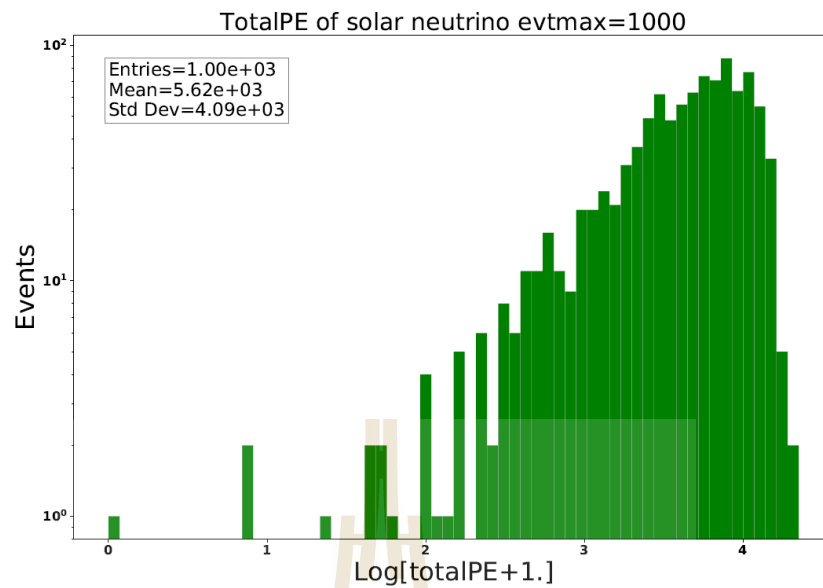


Figure 4.9 The histogram of the total number of PE from solar neutrino channel Be8. The mean of PE numbers is 5.62×10^3 and the standard deviation of this plot is 4.09×10^3

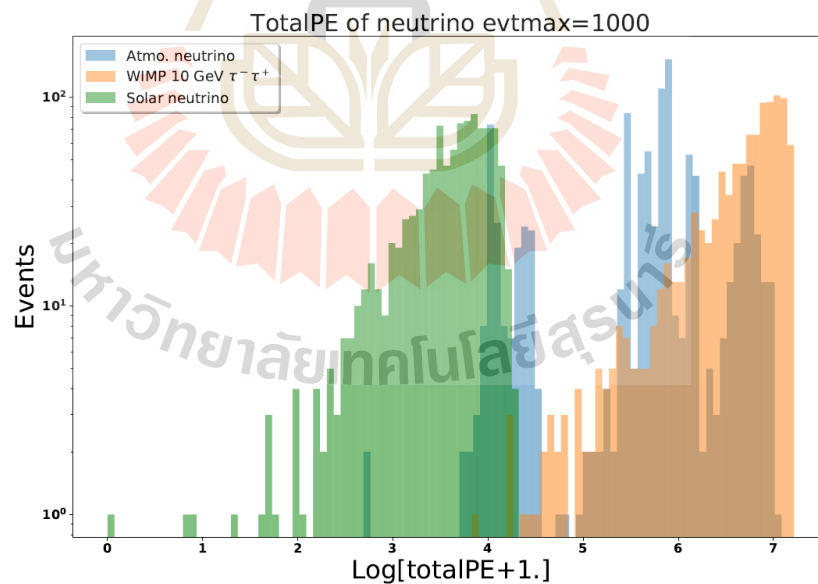


Figure 4.10 The histogram of the total number of PE in each event and from different sources, blue: atmospheric neutrino, orange: WIMPs mass equal to 10 GeV, and green: solar neutrino (channel Be8)

In Figure 4.10 illustrates the different shapes of the histogram from different sources. The atmospheric neutrino events provide a wide range of the total PE number which response neutrino interaction with LS. It discusses neutrino interacted via CC interaction with LS and produced several leptons and hadrons. The neutrino from captured WIMPs and solar neutrino consider only neutrino–electron scattering. It causes that the distribution of total PE number is in a smaller range than an atmospheric neutrino. Most of the neutrino events from solar capture WIMPs annihilation give many total PE numbers. The total number of PE from solar neutrino is lower than other because their energy is less than 20 MeV. Thereby, the total PE number rely on the neutrino interaction with LS and neutrino energy.

After neutrino collides LS, it gains the energy on LS and emits the photon that can be referred to as neutrino energy. However, we must consider more about the energy loss to an environment before the photon emitting in the vertex reconstruction method. In Figure 4.11, 4.12, 4.13 demonstrate deposited energy from different neutrino source by neutrino hitting LS, captured WIMPs mass equal to 10 GeV, atmospheric neutrino and solar neutrino, respectively, and compared three histograms in one plot on Figure 4.14.

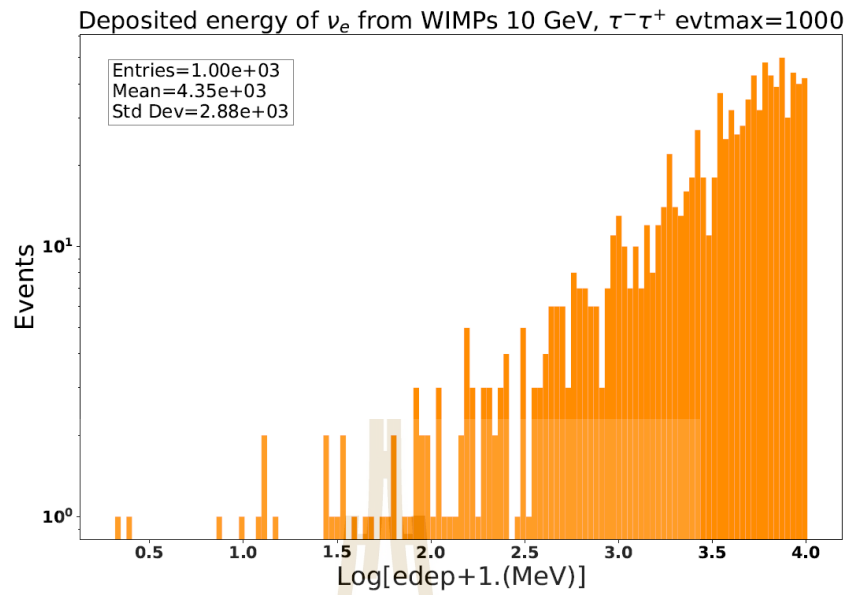


Figure 4.11 The histogram of deposited energy in MeV from captured WIMPs mass equal to 10 GeV. The mean energy of deposition is 4.35×10^3 MeV and the standard deviation of this plot is 2.88×10^3 MeV.

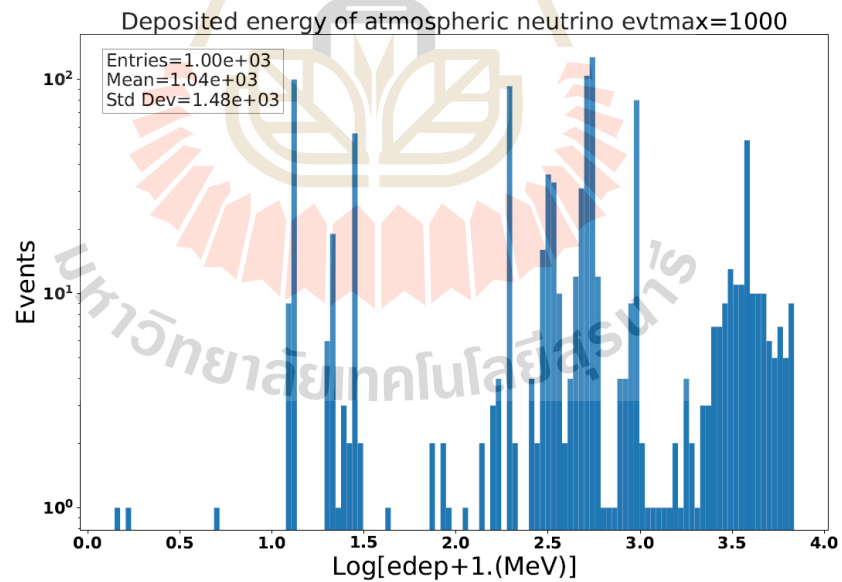


Figure 4.12 The histogram of deposited energy in MeV from atmospheric neutrino. The mean energy of deposition is 1.04×10^3 MeV and the standard deviation of this plot is 1.48×10^3 MeV.

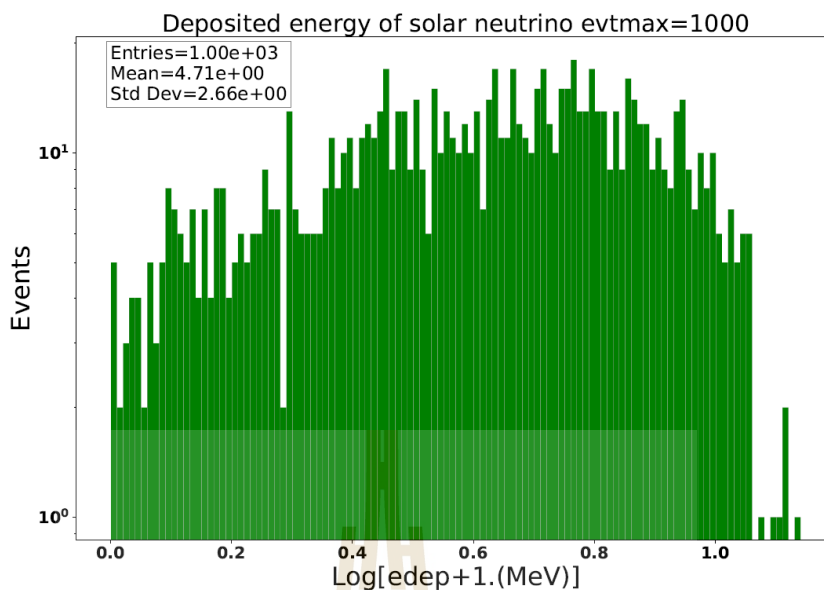


Figure 4.13 The histogram of deposited energy from solar neutrino channel Be8. The mean energy of deposition is 4.71 MeV and the standard deviation of this plot is 2.66 MeV.

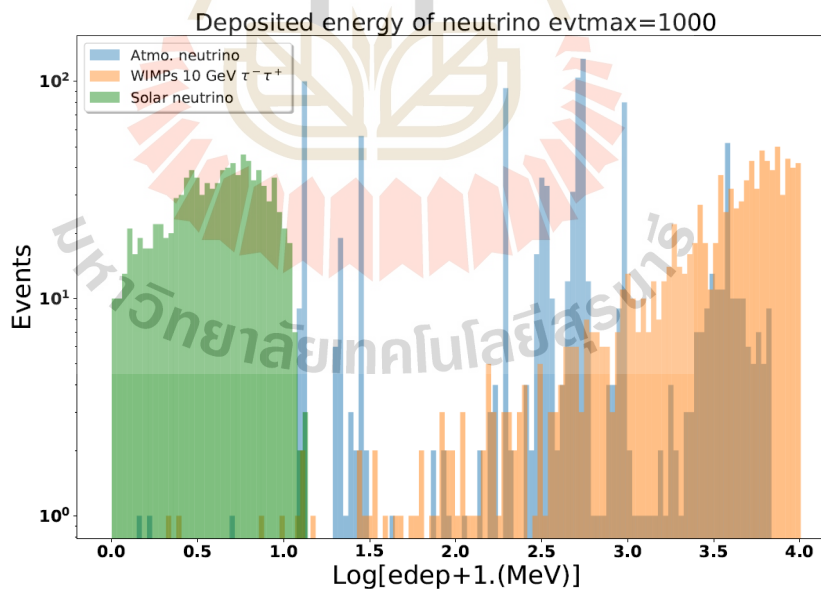


Figure 4.14 The histogram of deposited energy in MeV from different sources, blue: atmospheric neutrino, orange: WIMPs mass equal to 10 GeV, and green: solar neutrino (channel Be8)

The edep of atmospheric neutrino and neutrino from captured WIMPs provide broad range of energy due to their high neutrino energy. The distribution of edep from our source depends on an evaluation of kinetic electron energy by condition of the interacted cross-section which most of neutrino events offer high edep. The maximum edep in each source is related to maximum neutrino energy spectrum. The high edep provide many the total number of PE. We can separate our neutrino signal from solar neutrino by a search for high edep and numerous number of PE on PMTs. Although, the total number of PE and edep from atmospheric neutrino are difficult to distinguish from our signal, we can select a short range to consider number of events, for example, around more than 10^3 MeV, the atmospheric neutrino event is smaller than our signal. The atmospheric neutrino always takes place from cosmic ray interact with atmosphere of earth hence, if we do vertex reconstruction to determine time resolution, fired position on a detector and neutrino oscillation, we presumably describe the direction of the signal where it comes from.

Both of the above results are significant for vertex reconstruction. The number PE yield per edep can be obtained a function of vertex position (An et al., 2016) and visible energy (Lin et al., 2016). The vertex resolution depends on PMT time resolution (An et al., 2016) which is related to timing information. For this reason, the hit time of PE is also a important parameter for PMTs responding (Lin et al., 2016) and the hit time of PE from captured WIMPs mass equal to 10 GeV, atmospheric neutrino and solar neutrino are illustrated in Figure 4.15, 4.16, and 4.17, respectively.

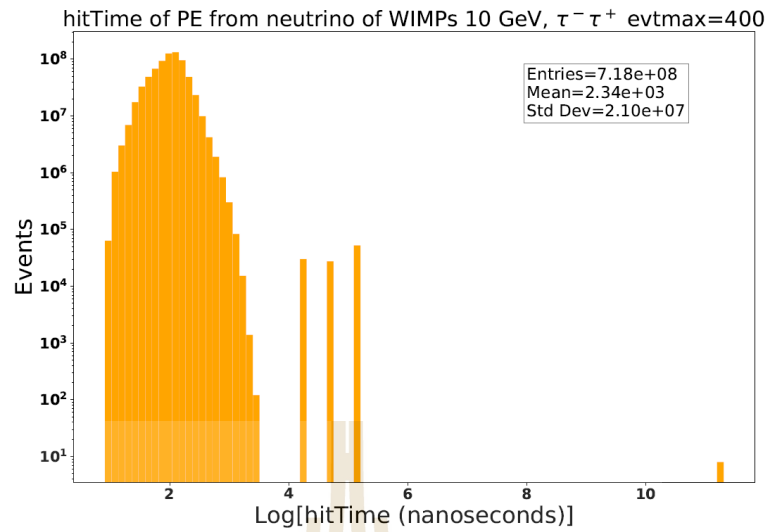


Figure 4.15 The histogram of hit time of PE hitting PMT in nanosecond from captured WIMPs mass equal to 10 GeV. The mean of hit time is 1.5×10^8 nanoseconds and the standard deviation is 5.91×10^{10} nanoseconds.

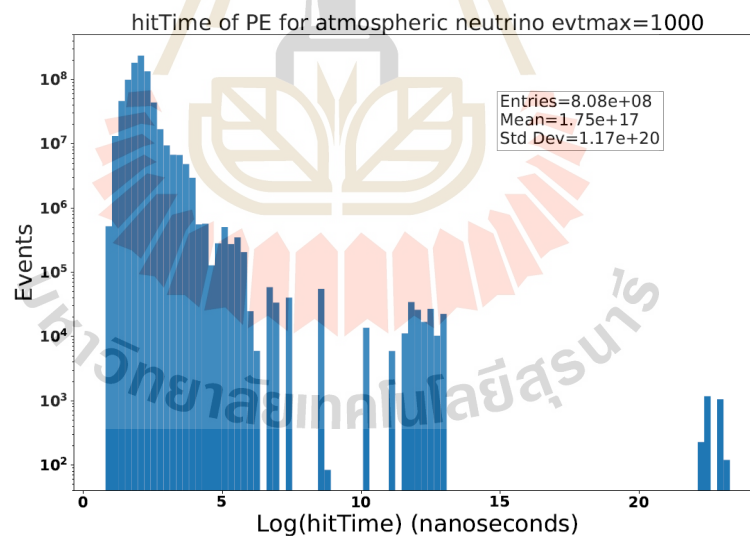


Figure 4.16 The histogram of hit Time of PE hitting PMT in nanosecond from an atmospheric neutrino. The mean of hit time is 1.75×10^{17} nanoseconds and the standard deviation is 1.17×10^{20} nanoseconds.

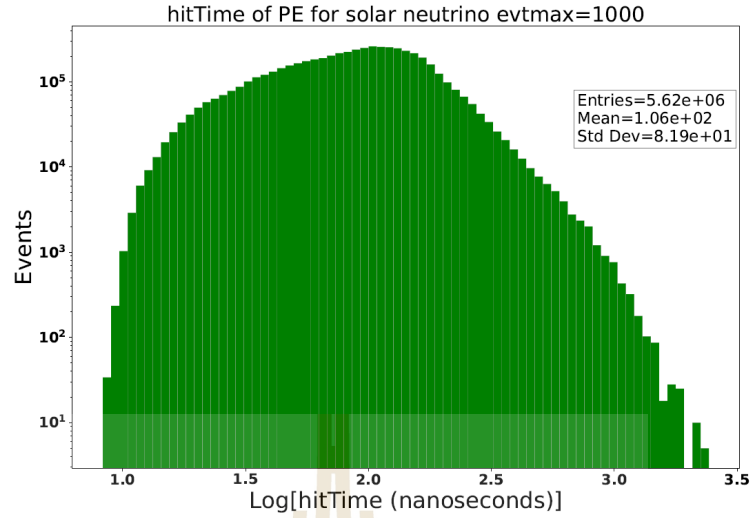


Figure 4.17 The histogram of hit Time of PE hitting PMT in nanosecond from solar neutrino channel Be8. The mean of hit time is 1.06×10^2 nanoseconds and the standard deviation is 81.9 nanoseconds.

The high neutrino energy produces more optical photon as well as the number of PE thus our neutrino give many numbers of PE for 1 neutrino event on detector simulation. Due to the limitation of memory and numerous PE number, we can plot the histogram of hit time from solar captured WIMPs merely 400 neutrino events in one plot. The hit time of PE for our signal is similar to hit time from solar neutrino in the range of 10–1,000 nanoseconds. The hit time of atmospheric neutrino extends to 10^{20} nanosecond. The JUNO software framework determine the neutrino energy in range MeV to ~ 10 GeV. We try to integrate more WIMPs mass in 100 GeV and 1,000 GeV and found that is a long time to run detector simulation and there is the upper boundary of PE number 2×10^6 per one run which does not rely on the number of neutrino events (- - evtmax). The solution of this problem is that turn off the optical mode but we cannot do reconstruction with this result and we will figure out in future work.

When the optical mode is turned off, the number of PE is an equal number

of events and the edep of neutrino from captured WIMPs mass equal to 100 and 1,000 GeV with dominated annihilated channel $\tau^-\tau^+$ display in Figure 4.18 and 4.19, respectively. The edep is high according to the neutrino energy. The shape of histogram of edep from captured WIMPs mass equal to 100 GeV is similar to WIMPs mass equal to 10 GeV in Figure 4.7. In Figure 4.19 demonstrates that events reduce at high edep more than 10^5 MeV because the edep is referred to electron energy which transfer from neutrino colliding LS and interaction is influenced by this process.

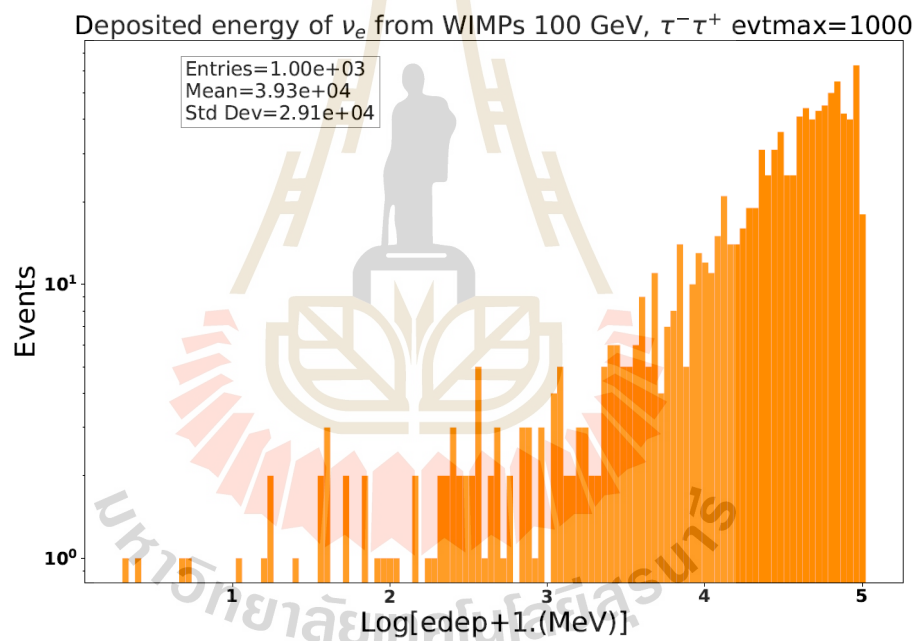


Figure 4.18 The histogram of deposited energy from captured WIMPs mass equal to 100 GeV.

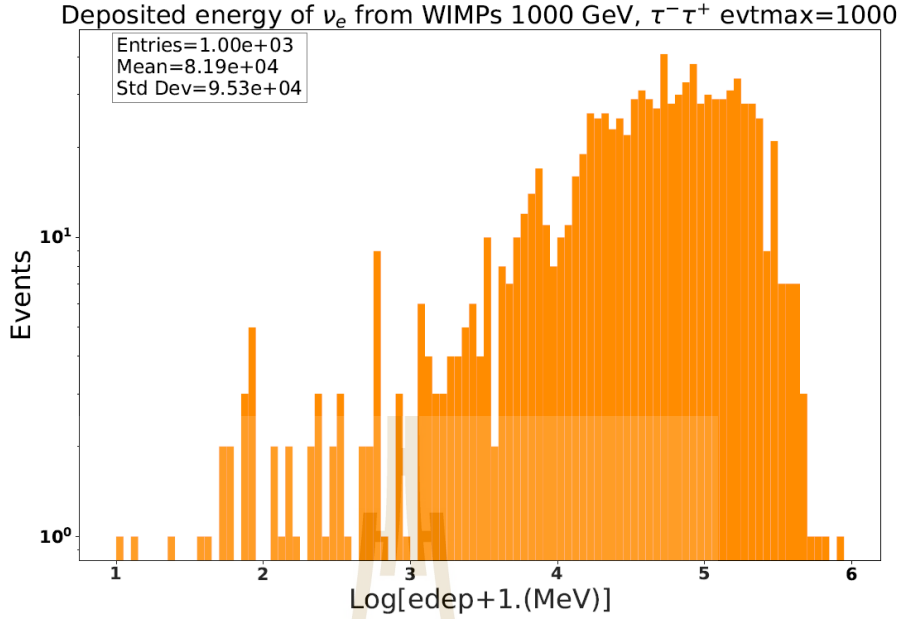


Figure 4.19 The histogram of deposited energy from captured WIMPs mass equal to 1,000 GeV.

An et al., 2016 calculated the atmospheric neutrino for electron neutrino events per 10 years on JUNO detector is 6,637 events for E_ν less than 20 GeV hence, the number of atmospheric neutrino events is 3,318 events per 5 years. The deposited energy of atmospheric neutrino events shows in the range of 0–6.82 GeV in Figure 4.12. The atmospheric neutrino energy spectrum exponentially decreases with primary cosmic ray energy spectrum ($E^{-2.7}$). Therefore, the number of atmospheric neutrino events reduce at high neutrino energy. We can estimate the atmospheric neutrino events in average energy range to compare with neutrino events from the WIMP signal. The sensitivity to σ_{XP}^{SD} for the 2σ significance of 5 years exposure time is (An et al., 2016)

$$\frac{s}{\sqrt{s+b}} = 2 \quad (4.1)$$

Where s is neutrino events from solar captured WIMPs annihilation, b is atmospheric neutrino events and 2 refers to 2σ detection significance. The b equals

to 3,318 events thus s equals to 117 events for 2σ .

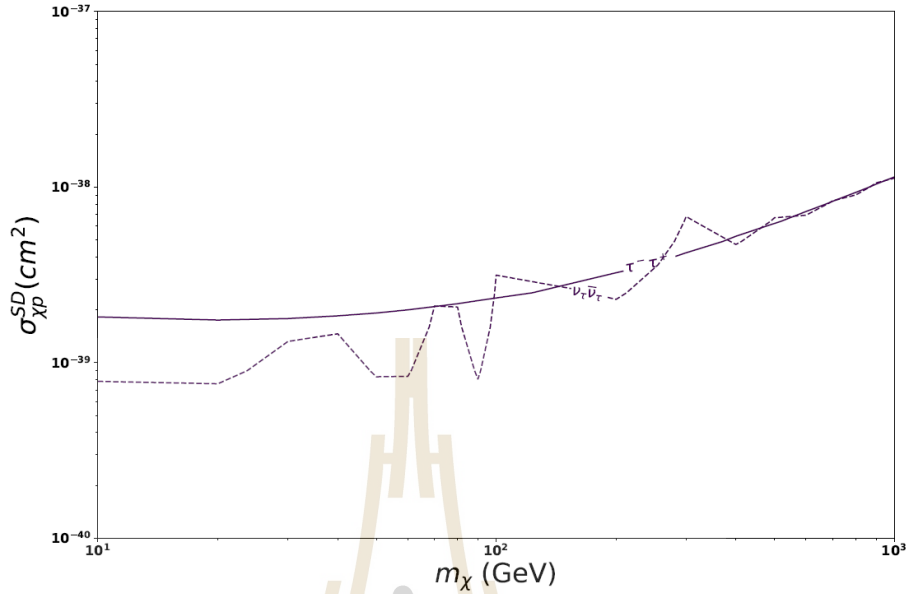


Figure 4.20 The JUNO 2σ sensitivity in 5 years to the SD cross section $\sigma_{\chi p}^{SD}$ in 5 years. The solid line is $\tau^- \tau^+$ channel and dashed line is $\nu_\tau \bar{\nu}_\tau$ channel.

The result of our plot in Figure 4.20 shows that the JUNO detector could detect neutrinos from WIMPs signal with $\sigma_{\chi p}^{SD}$ in the range of $7 \times 10^{-40} - 2 \times 10^{-39} \text{ cm}^2$ that depend on the annihilated channel and WIMPs mass. The fluctuation of graph in the $\nu_\tau \bar{\nu}_\tau$ channel is from the neutrino energy spectrum at E_ν closed to m_χ . The massive WIMPs provides less neutrino events thus $\sigma_{\chi p}^{SD}$ increases for more neutrino events. An et al. (2016) illustrates that $\sigma_{\chi p}^{SD}$ is 10^{-39} for m_χ in the range of 10–20 GeV and annihilated channels are $\nu\bar{\nu}$ and $\tau^- \tau^+$. Our calculation is slightly different from An et al. (2016). Our signal allows $\sigma_{\chi p}^{SD}$ less than from direct WIMPs search: XENON100 experiment which represents minimum SD WIMPs–proton cross section of $3.5 \times 10^{-38} \text{ cm}^2$ at WIMPs mass of $30 \text{ GeV}/c^2$ (Aprile et al., 2013). The recent experiment from XENON1T (Aprile et al., 2019) and PICO–60 (Amole et al., 2019) constrain that $\sigma_{\chi p}^{SD}$ is $2 \times 10^{-40} \text{ cm}^2$ for WIMPs mass equal to 30 GeV and $\sigma_{\chi p}^{SD}$ is $2.5 \times 10^{-41} \text{ cm}^2$ for WIMPs mass equal to 25 GeV, respectively. Both

of them have lower limit than us but the XENON1T reported no WIMPs signal and PICO-60 is also not insisting to detect WIMPs signal. The low σ_{xp}^{SD} has to consider carefully the BG from gamma-ray and neutrons.



CHAPTER V

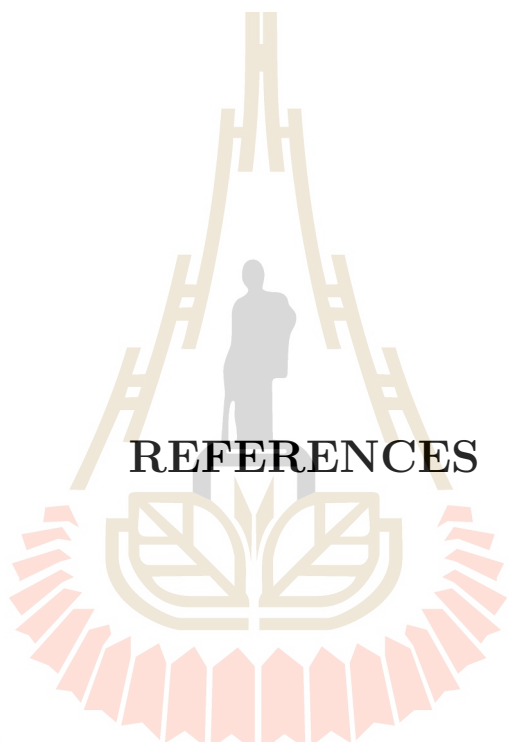
CONCLUSION

The best advantage of an observed neutrino is weak interaction. They rarely are interacted by other particles thus they are not contaminated by field, particles and physical process and then they can be traced back to their sources. The number of the low energetic neutrino events from low mass of WIMPs annihilation to neutrinos in GC is around 4 events per 10 years which is a few events to compare the BG. The neutrino events from captured WIMPs self-annihilation in the Sun's core depend on straightly the neutrino energy spectrum particularly direct neutrino annihilated channels. The massive WIMPs provide less neutrino event due to less number density. The 2σ detection level if we consider atmospheric neutrino as the main source of BG for 5 years observation, provide that $\sigma_{\chi P}^{SD}$ is $7.8 \times 10^{-40} \text{ cm}^2$ for WIMPs mass in the range of 10–20 GeV from tau neutrino channel. The JUNO experiment could receive neutrinos from a few lower $\sigma_{\chi P}^{SD}$ than direct WIMPs detection for XENON100. The current direct detection of PICO-60 constrain that upper limited of $\sigma_{\chi P}^{SD}$ is $4 \times 10^{-41} \text{ cm}^2$ for WIMPs mass in the range of 10–50 GeV but is not confirmed the WIMPs signal due to BG. However, JUNO sensitivity is better than some direct WIMPs detections, pending on the ability to distinguish it from BG events.

When the neutrino hit LS, our signal can be separated from other sources by deposited energy range and the number of PE. The solar neutrino provides low deposited energy hence our signal can be extracted from it. The atmospheric neutrino is ambiguous to dispart from our event on detector simulation. Never-

theless, we can do vertex reconstruction to determine particle position on CD and time profile on PMT and perhaps specify a source of neutrino event. The vertex reconstruction needs output file from detector simulation. When we consider captured WIMPs mass more than 10 GeV, the detector simulation generates a large number of PE and uses too many memories for one event. The limitation of this problem will be studied further, especially the vertex reconstruction method.

In Future work, we would like to extract our work in section 3.2 from solar neutrino generator to build DM generator which can set input arguments on the interface such as inputted file, neutrino–nucleon interaction, WIMPs mass, and channel from WIMPs self–annihilation. Nevertheless, firstly we have to solve simulation of exceedingly numerous PE numbers for massive WIMPs ($\gtrsim 10$ GeV) which cause minus PE ID and run for the long time and use extremely many memories. The solution of this problem may be vortex method for fast simulation by treating grid in CD sphere (Lin et al., 2016). Furthermore, the `user_detsim.root` which is a result from detector simulation is used in electronic simulation and vertex reconstruction as Figure 2.7. we can include the electronic simulation to affect electronic instrument before event reconstruction. The vertex reconstruction process determines the visible neutrino energy after colliding nuclei in LS. The method rechecks neutrino energy from neutrino spectrum which we input on physics generator. The JUNO experiment starts performing data collection in a few years thus the real events will be compared with simulated events inclusive neutrino sources, JUNO material, and the surrounding environment.



REFERENCES

มหาวิทยาลัยเทคโนโลยีสุรนารี

REFERENCES

- Amole, C., Ardid, M., Arnquist, I. J., Asner, D. M., Baxter, D., Behnke, E., Bressler, M., Broerman, B., Cao, G., Chen, C. J., Chowdhury, U., Clark, K., Collar, J. I., Cooper, P. S., Coutu, C. B., and et al. (2019). Dark Matter Search Results from the Complete Exposure of the PICO-60 C_3F_8 Bubble Chamber. **arXiv**.
- An, F., An, G., An, Q., Antonelli, V., Baussan, E., Beacom, J., Bezrukov, L., Blyth, S., Brugnera, R., Buizza Avanzini, M., Busto, J., Cabrera, A., Cai, H., Cai, X., Cammi, A., and et al. (2016). Neutrino physics with JUNO. **Journal of Physics G: Nuclear Physics**, 43: 030401.
- Aprile, E., Aalbers, J., Agostini, F., Alfonsi, M., Althueser, L., Amaro, F. D., Anthony, M., Antochi, V., Arneodo, F., Baudis, L., Bauermeister, B., Benabderrahmane, M. L., Berger, T., Breur, P. A., Brown, A., and et al. (2019). Constraining the spin-dependent WIMP-nucleon cross sections with XENON1T. **Physical Review Letters**, 122.
- Aprile, E., Alfonsi, M., Arisaka, K., Arneodo, F., Balan, C., Baudis, L., Bauermeister, B., Behrens, A., Beltrame, P., Bokeloh, K., Brown, A., Brown, E., Bruno, G., Budnik, R., Cardoso, J. M. R., and et al. (2013). Limits on spin-dependent WIMP-nucleon cross sections from 225 live days of XENON100 data. **Physical Review Letters**, 111.
- Bahcall, J. N., Kamionkowski, M., and Sirlin, A. (1995). Solar neutrinos: Radiative corrections in neutrino - electron scattering experiments. **Physical Review Journals**, D51.

- Bahcall, J. N., Serenelli, A. M., and Basu, S. (2005). New Solar Opacities, Abundances, Helioseismology, and Neutrino Fluxes. **IOP Publishing**, 621.
- Blennow, M., Edsjo, J., and Ohlsson, T. (2008). Neutrinos from WIMP Annihilations Obtained Using a Full Three-Flavor Monte Carlo Approach. **Journal of Cosmology and Astroparticle Physics**, 2008: 021.
- Clemens, D. P. (1985). Massachusetts-stony brook galactic plane CO survey - the galactic disk rotation curve. **Astrophysical Journal**, 295: 422–428.
- Drees, M. and Gerbier, G. (2015). DARK MATTER. Retrieved September, 2015, from <http://pdg.lbl.gov/2015/reviews/rpp2015-rev-dark-matter.pdf/>.
- Edsjo, J. (2007). Calculation of neutrino cross sections and the nusigma neutrino-nucleon scattering Monte Carlo, from <http://wimpsim.astroparticle.se/code/nucross3.pdf>.
- Edsjo, J., Bringmann, T., Gondolo, P., Ullio, P., Bergstrom, L., Schelke, M., Baltz, A. E., and Duda, G. (2018). DarkSUSY darksusy-6.1.0 Manual and description of routines, from <http://staff.fysik.su.se/~edsjo/darksusy/docs/Manual.pdf>.
- Edsjo, J. and Elevant, J. and Niblaeu, C. (2017). WIMPSIM 4.01:WIMPANN, solar crnu and WIMPEVENT Simulation of WIMP annihilations in the Earth/Sun, solar atmospheric neutrinos and propagation to a neutrino telescope, from <http://wimpsim.astroparticle.se/code/wimpsim-4.01.pdf>.
- Goodstein, D. (2012). Adventures in Cosmology. **Singapore: World Scientific Publishing Co. Pte. Ltd.**

- Jungman, G., Kamionkowski, M., and Griest, K. (1996). Supersymmetric dark matter. **Physics Reports**, 267.
- Lin, T. (2016). JUNO offline data processing process. (online) Available: http://juno.ihep.ac.cn/~offline/Doc/detsim/preq_processing.html.
- Lin, T., Deng, Z.-Y., Li, W.-D., Cao, G.-F., You, Z.-Y., and Li, X.-Y. (2016). Fast Muon Simulation in the JUNO Central Detector. **Chinese Physics**, C40.
- Majumdar, D. (2015). DARK MATTER An Introduction. **CRC Press**.
- Nesti, F. and Salucci, P. (2013). The Dark Matter halo of the Milky Way, AD 2013. **Journal of Cosmology and Astroparticle Physics**, 7.
- Overduin, M. J. and Wesson, S. P. (2008). THE LIGHT/DARK UNIVERSE Light from galaxies, Dark matter and Dark Energy. **Singapore: World Scientific Publishing Co. Pte. Ltd.**
- Palomares-Ruiz, S. and Pascoli, S. (2008). Testing MeV dark matter with neutrino detectors. **Physical Review Journals**, D77: 025025.
- Roszkowski, L., Sessolo, E. M., and Trojanowski, S. (2018). WIMP dark matter candidates and searches—current status and future prospects. **Reports on Progress in Physics**, 81: 066201.
- Vogel, P. and Beacom, J. F. (1999). Angular distribution of neutron inverse beta decay, anti-neutrino(e) + p \rightarrow e+ + n. **Physical Review Journals**, D60.
- Wechakama, M. (2013). Multi-messenger constraints and pressure from dark matter annihilation into e- and e+ pairs, from

http://inspirehep.net/record/1260513/files/wechakama_diss.pdf.

Ph.D. Thesis. The University of Potsdam.

Wechakama, M. and Ascasibar, Y. (2014). Multimessenger constraints on dark matter annihilation into electron-positron pairs. **Monthly Notices of the Royal Astronomical Society**, 439.

Widmark, A. (2016). Dark Matter Capture by the Sun via Xelf-Interaction. **Master Degree Thesis.** Chalmers University of Technology.

Wurm, M. (2017). Experimental neutrino physics. (online) Available: <http://www.staff.uni-mainz.de/wurmm/juno.html>.



CURRICULUM VITAE

NAME: Jaruchit Siripak **GENDER:** Female

NATIONALITY: Thai **DATE OF BIRTH:** April 11, 1994

EDUCATIONS:

- 4 July 2016 Bachelor Degree of Science in Physics (First Class Honors), Suranaree University of Technology

PUBLICATIONS:

- The conference on Siam Physics Congress 2018 (SPC 2018) in the topic of “Simulation of neutrino signal from dark matter annihilation for JUNO experiment” during 21–23 May 2018 at Phitsanulok, Thailand.

AWARDS:

-

GRANTS AND FELLOWSHIPS:

- Received the scholarship of The Development and Promotion of Science and Technology Talents project (DPST Scholarship), Ministry of Science and Technology, since 2012–present.

POSITION AND PLACE OF WORK:

-